LabelAny3D: Label Any Object 3D in the Wild

Jin Yao[*] **Radowan Mahmud Redoy**[*] **Sebastian Elbaum** **Matthew B. Dwyer** **Zezhou Cheng**
University of Virginia
https://uva-computer-vision-lab.github.io/LabelAny3D/

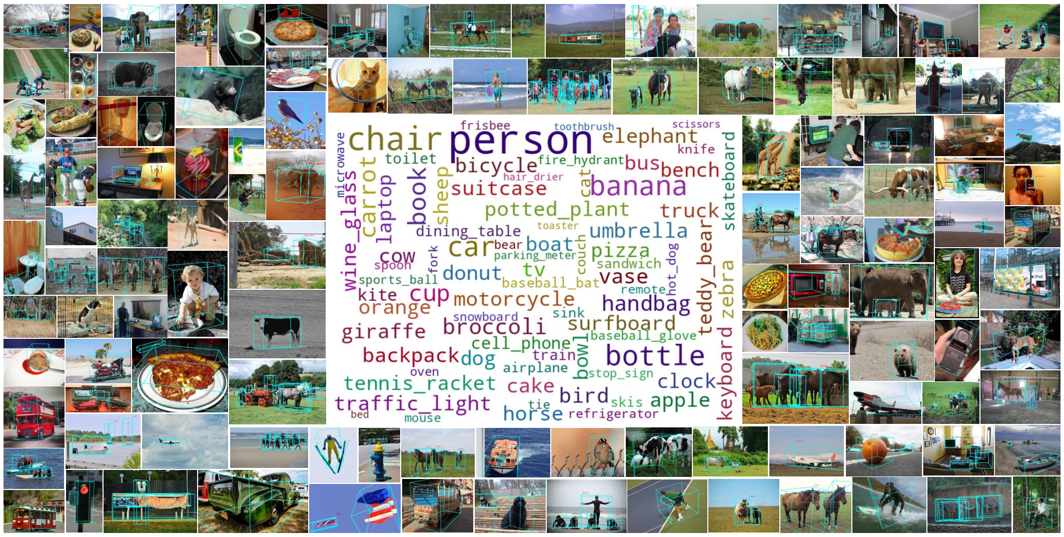

Figure 1: Samples from our proposed COCO3D benchmark.

Abstract

Detecting objects in 3D space from monocular input is crucial for applications ranging from robotics to scene understanding. Despite advanced performance in the indoor and autonomous driving domains, existing monocular 3D detection models struggle with in-the-wild images due to the lack of 3D in-the-wild datasets and the challenges of 3D annotation. We introduce **LabelAny3D**, an *analysis-by-synthesis* framework that reconstructs holistic 3D scenes from 2D images to efficiently produce high-quality 3D bounding box annotations. Built on this pipeline, we present **COCO3D**, a new benchmark for open-vocabulary monocular 3D detection, derived from the MS-COCO dataset and covering a wide range of object categories absent from existing 3D datasets. Experiments show that annotations generated by LabelAny3D improve monocular 3D detection performance across multiple benchmarks, outperforming prior auto-labeling approaches in quality. These results demonstrate the promise of foundation-model-driven annotation for scaling up 3D recognition in realistic, open-world settings.

1 Introduction

Monocular 3D object detection—recognizing and localizing objects in 3D space from a single RGB image—is an emerging research direction with wide-ranging applications in robotics, autonomous driving, and embodied AI. Compared to approaches that rely on specialized sensors such as LiDAR

[*] Equal contribution

39th Conference on Neural Information Processing Systems (NeurIPS 2025).

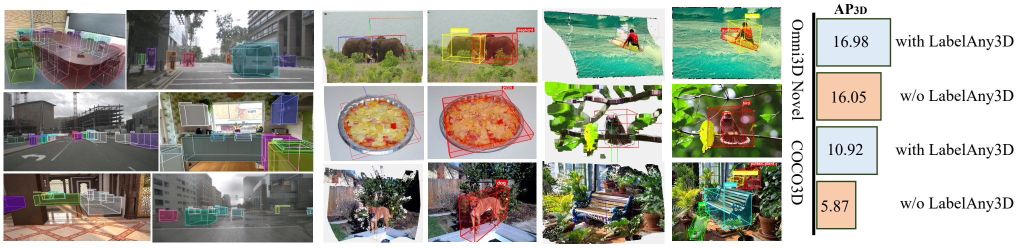

(a) Omni3D: indoor or self-driving (b) 3D annotations from LabelAny3D (c) Monocular 3D Detection

Figure 2: **Overview.** **(a)** Omni3D [7] offers large-scale 3D annotations but primarily covers indoor and self-driving scenarios. **(b)** The proposed LabelAny3D reconstructs 3D scenes (left) to annotate objects in 3D (right). **(c)** Leveraging LabelAny3D pseudo-labels to train a monocular 3D detector raises its AP_{3D} (average precision; higher is better) on both Omni3D novel categories [75] and our new COCO3D benchmark.

or multi-view stereo [46, 47, 11, 12, 77, 84, 80, 79, 52, 20], monocular methods are lightweight, accessible, and energy-efficient, making them well-suited for many real-world deployments (*e.g.*, AR/VR wearables). Recent advances such as Cube R-CNN [7] have achieved strong 3D detection performance by training on large, high-quality datasets, while OVMono3D [75] extends this task to the open-vocabulary setting, aiming to detect arbitrary object categories in 3D from monocular views.

Despite progress, a critical bottleneck has been highlighted in recent works [7, 75, 22, 27]: the need for large-scale 3D datasets with high-quality 3D bounding box annotations for effective training and evaluation. This aligns with a broader trend observed in vision and language foundation models [1, 44, 60]: performance improves significantly with more diverse, realistic training data and high-quality supervision. However, unlike 2D image recognition or language tasks, existing 3D datasets [8, 23, 7, 4, 15] are still constrained in scalability, scene diversity, and geometric complexity. As illustrated in Figure 2a, Omni3D [7]—currently the largest public dataset—is dominated by indoor [15, 4, 63, 2, 58] and autonomous driving scenes [24, 9], with limited coverage of common objects (*e.g.*, animals). These constraints hinder both the training and evaluation of generalizable monocular 3D detectors. While prior works [7, 75, 78] demonstrate qualitative success on in-the-wild images from MS-COCO [40], the lack of 3D annotations prevents systematic and quantitative benchmarking. This motivates the central question in this work: *how can we produce high-quality 3D annotations on natural images with minimal human supervision?*

Two major challenges limit scalable 3D dataset construction. First, *collecting 3D data is expensive*: in-the-wild images rarely include depth, and LiDAR or depth sensors require costly hardware and careful calibration, making them far less scalable than RGB capture. Second, *annotating 3D data is labor-intensive*: labeling 3D bounding boxes requires significantly more effort than 2D annotations. Several prior works have attempted to address these issues. For instance, OVM3D-Det [27] lifts 2D images into 3D using off-the-shelf *metric* depth estimation models [53, 6] to generate pseudo-LiDAR data, and infer 3D bounding boxes using object size priors from large language models (*e.g.*, average height for a pedestrian is 1.7 meters). While effective for objects with consistent sizes (*e.g.* cars), this approach struggles with categories exhibiting high intra-class variations (*e.g.*, baby *vs.* adult elephant). It also relies heavily on accurate metric depth prediction—a task that remains fundamentally ill-posed when relying solely on 2D input, as object appearance is entangled with both focal length and actual distance to the camera. Another approach, 3D Copy-Paste [22], augments 3D annotations by inserting synthetic 3D models into images, which however induces the sim-to-real challenge.

To address these limitations, we propose LabelAny3D, an automatic 3D annotation pipeline that efficiently generates 3D bounding boxes for objects across arbitrary categories. Unlike prior works [22, 27], LabelAny3D adopts an *analysis-by-synthesis* paradigm: it reconstructs the holistic 3D scene from monocular images and uses the synthesized representation to infer spatially consistent 3D object annotations (Figure 2b and 3). Our framework is motivated by three key observations: (1) although metric depth estimation remains ill-posed, relative depth estimation [66] is significantly more reliable and consistent; (2) recent advances in object-centric 3D reconstruction, powered by large-scale 3D shape datasets [17] and generative modeling techniques [72], have enabled accurate shape recovery; and (3) 2D vision foundation models [33, 44] offer strong generalization capabilities across diverse, in-the-wild visual domains.

By integrating diverse vision foundation models, LabelAny3D produces high-quality 3D annotations suitable for training monocular 3D models and constructing benchmarks with minimal human supervision. Our experiments demonstrate that the 3D annotations from our pipeline lead to consistent improvements in monocular 3D detection across multiple benchmarks (Figure 2c), outperforming existing auto-labeling methods [27]. We further introduce COCO3D, a new benchmark curated from MS-COCO [40] validation images using our pipeline with human refinement, covering a wide variety of everyday object categories encountered in the wild, as presented in Figure 1.

In summary, our key contributions are as follows:

- We introduce LabelAny3D, an efficient 3D annotation pipeline that generates high-quality 3D bounding boxes on in-the-wild images in an *analysis-by-synthesis* manner.
- We demonstrate that 3D annotations from LabelAny3D consistently improve monocular 3D detection performance, surpassing existing auto-labeling approaches.
- We curate COCO3D, a new benchmark for open-vocabulary monocular 3D detection, featuring a diverse range of object categories beyond those covered in existing 3D datasets.

2 Related work

3D Datasets. Many datasets have been developed to support 3D detection. KITTI [23] and nuScenes [8] focus on autonomous driving, offering LiDAR and camera data for object detection and tracking in urban environments. SUN RGB-D [63], Hypersim [58] and ARKitScenes [4] target indoor settings, capturing room-scale layouts with depth and semantic annotations. Objectron [2] leverage mobile devices to collect real-world 3D object scans, enabling fine-grained object-centric learning. Omni3D [7] unifies multiple datasets to create a large-scale benchmark for general 3D object detection, yet existing benchmarks remain limited in their coverage of diverse, open-world scenarios. In contrast, we propose to extend 3D datasets beyond indoor and autonomous driving domains. This enables broader generalization across diverse, in-the-wild scenarios.

Monocular 3D Detection. Early studies on this task focused predominantly on specialized applications within either outdoor [14, 82, 83, 68, 13, 81, 26, 67] or indoor environments [16, 28, 49, 61, 35], particularly targeting autonomous driving and room layout estimation. The Omni3D dataset facilitated Cube R-CNN [7] in pioneering unified monocular 3D detection. Subsequently, UniMODE [39] extended these advances by proposing the first successful BEV-based detector applicable across diverse environments. Despite these achievements, most existing methods are constrained by closed vocabularies. Recent advancements in open-vocabulary 3D detection [46, 47, 11, 12, 77, 84, 80, 79, 52, 20, 69] primarily focus on utilizing 3D point clouds, while OVMono3D [75] first explores the open vocabulary 3D detection task with only monocular image as input. DetAny3D [78] further boosts performance through superior 2D priors and extensive training data. However, these models still face challenges with generalization to in-the-wild imagery like MS-COCO [40], highlighting the ongoing issue of domain coverage limitations in training datasets.

Label-efficient 3D Detection. Due to the high cost of 3D labeling, previous studies have investigated approaches to reduce the reliance on 3D supervision in monocular 3D detection tasks [27, 71, 31, 10, 25]. For instance, Huang *et al.* [27] utilizes open-vocabulary 2D models and pseudo-LiDAR to automatically annotate 3D objects in RGB images, while 3D Copy-Paste [22] inserts synthetic 3D object shapes into 2D images to augment 3D annotations. Additionally, SKD-WM3D [31] introduces a weakly-supervised monocular 3D detection framework by distilling knowledge from pre-trained depth estimation models. While these weakly-supervised methods have proven effective, their application is often limited to indoor or autonomous driving contexts. In this work, we aim to develop novel techniques to broaden the domain coverage of 3D detection models.

Model-in-the-loop Data Labeling. Model-in-the-loop data labeling leverages foundation models to enhance and accelerate data annotation. Prior works have explored this methodology across various tasks. Stereo4D [32] utilizes stereo depth estimation [42] and 2D tracking [19] models to construct 3D trajectory datasets. Cap3D [48] employs vision-language models such as BLIP2 [38], CLIP [54], and GPT-4 [1] to develop a scalable pipeline for captioning 3D assets. DynPose [59] creates dynamic camera pose datasets by integrating advanced tracking [19] and masking [55, 29] models. Unlike these approaches, our work focuses on the task of 3D bounding box annotation from single-view images. By incorporating advanced models, such as monocular depth estimation [66, 6] and image-to-3D reconstruction [72], our pipeline enables accurate and efficient 3D labeling.

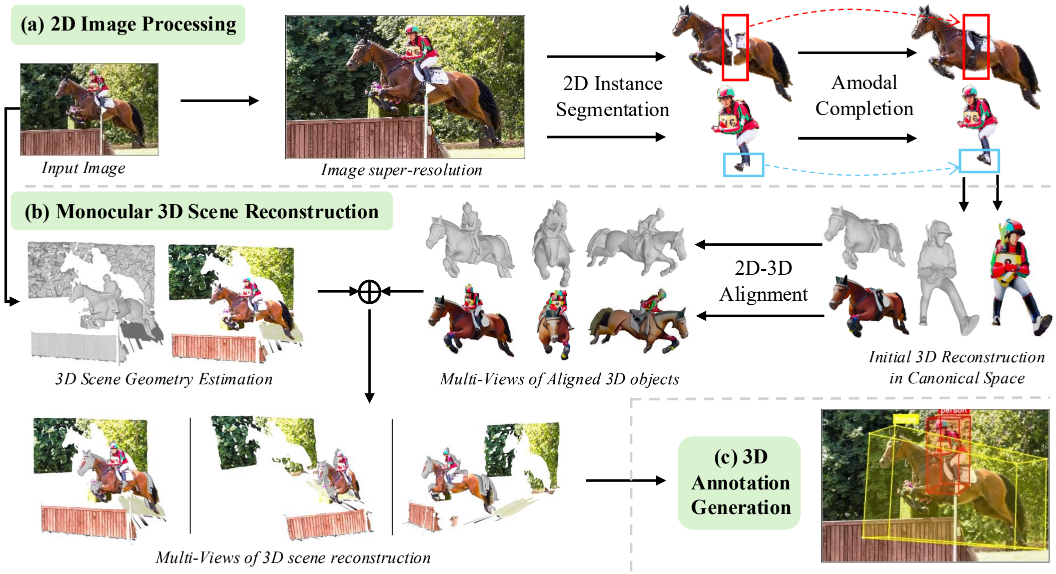
(a) 2D Image Processing
Input Image
Image super-resolution
2D Instance Segmentation
Amodal Completion
(b) Monocular 3D Scene Reconstruction
3D Scene Geometry Estimation
Multi-Views of Aligned 3D objects
2D-3D Alignment
Initial 3D Reconstruction in Canonical Space
Multi-Views of 3D scene reconstruction
(c) 3D Annotation Generation
person

Figure 3: **LabelAny3D**. **(a)** Given an image, we first extract high-resolution object crops; **(b)** A holistic 3D scene is then built from robust depth estimation, 3D object reconstruction, and 2D-3D alignment algorithms. **(c)** Lastly, 3D labels can be easily extracted from the reconstructed 3D scene.

3 LabelAny3D: Automatic 3D Labeling via 3D Reconstruction

This section details the proposed LabelAny3D annotation pipeline. As shown in Figure 3, the pipeline generates pseudo annotations from an input image through the following steps.

Image Super-resolution. Many objects in MS-COCO [40] appear at low resolution due to factors such as small object scale or compression artifacts, which poses challenges for downstream tasks like 3D reconstruction. To address this, we leverage InvSR [76], a diffusion-based super-resolution (SR) model, to enhance the input image by a factor of $\times 4$. This improves perceptual quality by recovering fine details and sharpening object boundaries. Given an input image $I \in \mathbb{R}^{H\times W\times 3}$, the enhanced image is $I^{\text{SR}} \in \mathbb{R}^{4H\times 4W\times 3}$.

2D Instance Segmentation. Prior studies have shown that the ground truth segmentation masks in MS-COCO [40] often exhibit annotation errors. To mitigate this, we leverage the COCONut dataset [18], which provides refined and high-quality segmentation masks built upon the MS-COCO [40] annotations. Given an image and its super-resolved version I^{SR}, we compute the intersection of each object mask M with a boundary mask and if the total intersection of an object exceeds a threshold, the object is considered truncated and excluded. Next, each mask M is upscaled to $M^{\text{SR}} \in \mathbb{R}^{4H\times 4W}$ using nearest-neighbor interpolation to match the resolution of I^{SR}. We also remove any object whose post-processed mask area is below a threshold, as such objects are too small for reliable geometry. Using I^{SR} and M^{SR} we extract the enhanced crop of the target object.

Amodal Completion & 3D Reconstruction. To handle occluded objects, we adopt an amodal completion strategy inspired by prior work in Gen3DSR [3]. We leverage the learned amodal completion diffusion model from Gen3DSR to inpaint the missing regions of the object crop, generating a completed version O_{comp} of the targeted object. With O_{comp} we apply single-view 3D reconstruction methods (*e.g.*, TRELLIS [72]) to recover the full 3D mesh in a canonical pose with normalized scale.

Scene Geometry Estimation. We utilize an *affine-invariant* representation of the scene geometry from MoGe [66], and another from a *metric depth estimation model*, such as Depth Pro [6]. To recover the 3D geometry, the MoGe depth map is aligned to the scale and perspective of the metric depth map which is considered to represent real-world geometry [5, 3]. This step ensures that the depth values from MoGe are scaled and transformed to match the metric scale and viewpoint of the target scene. Next, the aligned depth map is *unprojected* into 3D space using the camera intrinsic matrix provided by the MoGe model, to recover the full 3D structure of the target scene.

Pose Estimation via 2D-3D Alignment. After obtaining 2D object regions O_{comp} and 3D reconstructions, we localize the 3D objects within the scene by estimating its pose relative to the input image. This is achieved through dense correspondence matching between the real image and a set of rendered views of the object mesh Mesh_{sr}. We adopt MASt3R [37] to compute 2D-2D correspondences between the super-resolved real image and the rendered views. Let $x_0 \in \mathbb{R}^2$ denote pixel coordinates in the real image, and $x_1 \in \mathbb{R}^2$ in the rendered view. These matched keypoints are filtered near image borders and invalid depth regions. Using the rendered depth map along with known intrinsics and extrinsics from rendering, we unproject x_1 to obtain corresponding 3D points $X_c \in \mathbb{R}^3$ on the Mesh_{sr}. Given the resulting 3D–2D correspondences (X_c, x_0) and camera intrinsics K inferred from MoGe [66], we apply a Perspective-n-Point (PnP) solver [36] with RANSAC [21] to estimate the relative camera pose (R, T). The object is then transformed into the input image's coordinate frame using this pose, yielding a reconstruction aligned with the relative layout of the original scene.

Scale Estimation via Depth Alignment. To recover metric scale, we align the rendered object to the real scene using depth-based scale estimation. Specifically, given the binary mask M from segmentation and the rendered mask M_{render} obtained using the previously estimated pose, we compute an overlap region $\Omega = M \cap M_{\text{render}}$. Letting D_{real} and D_{render} denote the real and rendered depth maps from the same pose, respectively, we estimate the scale factor s as the median depth ratio:

$$s = \text{median}\left(\frac{D_{\text{real}}(\Omega)}{D_{\text{render}}(\Omega)}\right).$$

The estimated scale s is applied to the rotation and translation parameters to form the final transformation matrix. This transformation places the reconstructed 3D object into the metric-scale scene point cloud, completing the 3D scene reconstruction.

3D Annotation Generation. In this step, we uniformly sample a point cloud from the mesh surface, capturing the object's geometry in its posed state. As TRELLIS [72] generates objects in a canonical pose with the upright direction aligned to gravity, following prior works [27, 51], we align the vertical axis of the bounding box with this canonical upward direction. To estimate orientation and size, we project the point cloud onto the plane orthogonal to the upward axis and apply PCA to determine the dominant yaw. The point cloud is then rotated to align with the canonical axes, and a tight 3D bounding box is fitted around its extent. This yields the object's 3D bounding box attributes, including center position, orientation, and dimensions.

4 Downstream Applications

Section 4.1 introduces a new monocular 3D detection benchmark curated from MS-COCO [40]. Section 4.2 presents our training details using the pseudo labels generated by LabelAny3D.

4.1 COCO3D Benchmark

Human refinement. We apply LabelAny3D to curate a benchmark for evaluating (open-vocabulary) monocular 3D detection models. To ensure the high quality of our 3D annotations, we employ a human-in-the-loop refinement process. Five annotators with prior 3D vision experience refined the pipeline-generated labels by adjusting bounding box dimensions, rotation, and center position based on the generated point maps. They also had the option to remove any generated bounding box they deemed excessively noisy. In addition, the annotators performed a filtering step to exclude samples containing undesirable characteristics, such as reflections of objects on surfaces like mirrors, windows, or screens, as well as 2D posters or symbols representing 3D objects. Figure 4c presents a selection of diverse examples that were removed during this process. This refinement requires minimal manual effort, supporting efficient large-scale annotation.

Statistics. The COCO3D benchmark[2] comprises 2,039 human-refined images with a total of 5,373 instances spanning all 80 categories of the MS-COCO dataset [40]. Figure 1 illustrates samples of the final curated results, along with the categories represented in our COCO3D benchmark. We construct this benchmark using the validation set of the MS-COCO dataset. Figure 4a presents the distribution of the top 50 categories within the COCO3D benchmark. Notably, the *person* category in MS-COCO includes a wide range of examples featuring individuals in various poses, sizes, and

[2] A larger version 2 will be released soon. For this camera-ready version, we present results on version 1.

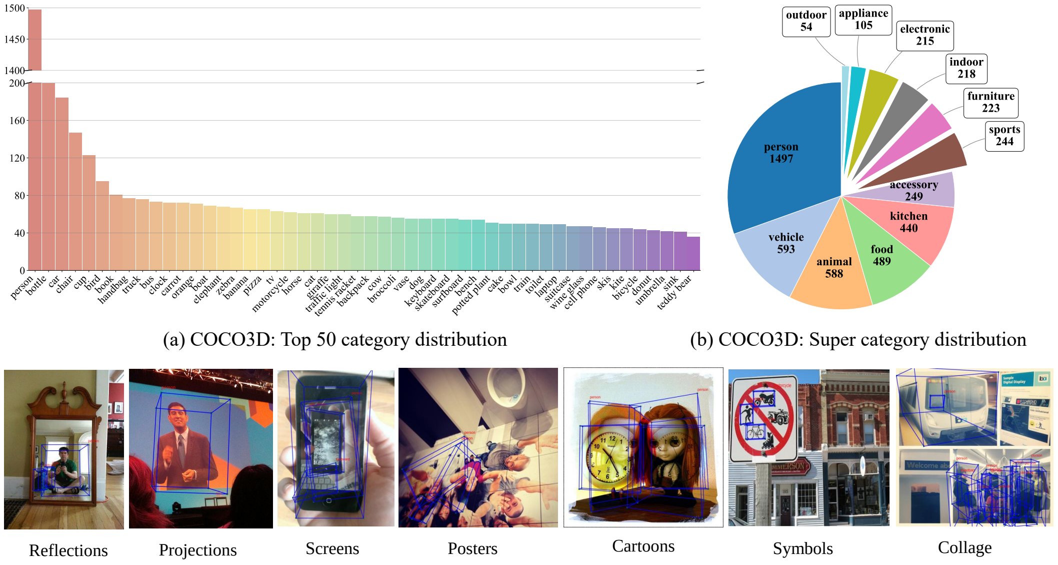

(a) COCO3D: Top 50 category distribution

(b) COCO3D: Super category distribution

(c) COCO3D: Removed photo samples during human refinement based on mentioned characteristics

Figure 4: **COCO3D benchmark. (a)** Distribution of the top 50 categories in the COCO3D benchmark. **(b)** Super-category-wise distribution in the COCO3D benchmark, based on MS-COCO [40]. **(c)** Examples of samples removed from COCO3D during the human refinement process.

age groups, contributing to a rich and diverse set of samples. Figure 4b displays the distribution of supercategories, further demonstrating the diversity captured by our benchmark.

4.2 Train Monocular 3D Detector with LabelAny3D

We build our model upon OVMono3D [75], a state-of-the-art open-vocabulary monocular 3D detection model. OVMono3D consists of two stages: (1) detecting and localizing objects in 2D using open-vocabulary detectors (*e.g.*, Grounding DINO [45]); and (2) lifting 2D bounding boxes to 3D cuboids in a class-agnostic manner. Specifically, given an image I, a text prompt T, and 2D bounding boxes with category labels from a 2D detector, OVMono3D extracts multi-scale feature maps from pretrained vision transformers (*e.g.*, DINOv2 [50]) for each 2D bounding box. These features are then processed by a feed-forward network to predict 3D attributes.

Training objective. We closely follow prior work [7] to train our models. We train only the lifting head of OVMono3D [75] using ground-truth 2D bounding boxes. The training objective of is defined as:

$$\mathcal{L} = \sqrt{2}\,\exp(-\mu)\,\mathcal{L}_{3\text{D}} + \mu, \tag{1}$$

where $\mathcal{L}_{3\text{D}}$ is the loss from the 3D cube head, and μ denotes the uncertainty score. The 3D loss $\mathcal{L}_{3\text{D}}$ consists of disentangled losses for each 3D attribute [62]:

$$\mathcal{L}_{3\text{D}} = \sum_{a} \mathcal{L}_{3\text{D}}^{(a)} + \mathcal{L}_{3\text{D}}^{\text{all}}, \tag{2}$$

where $a \in \{(x_{2\text{D}}, y_{2\text{D}}),\ z,\ (w, h, l),\ r\}$ denotes groups of 3D attributes: 2D center shift, depth, dimensions, and rotation. Each component loss $\mathcal{L}_{3\text{D}}^{(a)}$ isolates the error of a specific attribute group by substituting all other predicted variables with their ground-truth counterparts when constructing the predicted 3D bounding box $B_{3\text{D}}$. The holistic loss $\mathcal{L}_{3\text{D}}^{\text{all}}$ compares the predicted 3D bounding box with the ground truth using the Chamfer Loss:

$$\mathcal{L}_{3\text{D}}^{\text{all}} = \ell_{\text{Chamfer}}(B_{3\text{D}},\ B_{3\text{D}}^{\text{gt}}). \tag{3}$$

Training Data. We curate a training set of 15,869 images from the MS-COCO [40] training split, annotated using our LabelAny3D pipeline *without any human refinement*. This pseudo-labeled dataset is used to either train the OVMono3D model from scratch or fine-tune it. For fine-tuning, we

Table 1: **Performance of OVMono3D [75] with different training settings.** We report scores on our COCO3D benchmark, and the novel and base category splits of Omni3D in OVMono3D evaluation. The best results for each metric are highlighted in **bold**. The second best is underlined. "Rel" denotes the relative layout metrics. "*" denotes the model is initialized with the pretrained OVMono3D.

Training dataset	COCO3D				Omni3D Novel		Omni3D Base	
	$\text{AP}_{\text{3D}}\uparrow$	$\text{AR}_{\text{3D}}\uparrow$	$\text{AP}_{\text{3D}}^{\text{Rel}}\uparrow$	$\text{AR}_{\text{3D}}^{\text{Rel}}\uparrow$	$\text{AP}_{\text{3D}}\uparrow$	$\text{AR}_{\text{3D}}\uparrow$	$\text{AP}_{\text{3D}}\uparrow$	$\text{AR}_{\text{3D}}\uparrow$
Baseline: Omni3D [7, 75]	5.87	10.51	20.86	30.06	16.05	36.85	**24.77**	**47.28**
OVM3D-Det* [27]	2.69	5.25	7.98	12.25	5.30	15.71	7.32	26.34
Omni3D [7] + OVM3D-Det [27]	6.82	11.94	20.76	27.69	15.55	**37.18**	22.35	42.68
LabelAny3D	7.78	15.41	24.66	34.54	8.47	23.34	3.92	19.66
Omni3D [7] + LabelAny3D	**10.92**	**20.10**	**32.02**	**43.82**	**16.98**	36.96	22.74	42.46

initialize from the OVMono3D model pretrained on Omni3D [7] and further train it on the combined LabelAny3D and Omni3D datasets. For training from scratch, the model is trained solely on the LabelAny3D annotations without relying on any external ground truth 3D supervision.

5 Experiments

5.1 Experimental Setup

Benchmarks. LabelAny3D is evaluated on our COCO3D benchmark. In this benchmark, we exclude 10 of the 80 categories from evaluation due to either too few evaluation instances or extreme aspect ratios (*e.g.*, spoon, baseball bat). We also assess the open-vocabulary detection capabilities of our trained model on Omni3D [7], which primarily encompasses indoor datasets such as SUN RGB-D [63], ARKitScenes [4], and Hypersim [58]; the object-centric dataset Objectron [2]; and autonomous driving datasets including nuScenes [8] and KITTI [24].

Baselines. We evaluate LabelAny3D in terms of both pseudo annotation quality and its effectiveness for training open-vocabulary monocular 3D detectors. Specifically, we compare LabelAny3D with OVM3D-Det [27] on annotation quality and downstream detection performance. Additionally, using our curated COCO3D validation set, we benchmark the performance of OVMono3D [75] and OVMono3D fine-tuned on our pseudo annotations derived from the MS-COCO [40] training set.

Evaluations. Following [7, 75], we report mean AP_{3D} and AR_{3D}, computed using Intersection-over-Union (IoU) between predicted and ground-truth 3D bounding boxes across IoU thresholds ranging from 0.05 to 0.50 in increments of 0.05.

Since the metric depth in our COCO3D validation set is derived from model predictions, it may contain biases due to the inherent difficulty in accurately predicting and human-validating absolute depth. In contrast, the relative depth from MoGe [66] is rigorously verified through human refinement, providing greater reliability. To address this, we introduce a novel metric, *Relative Layout* AP_{3D}, within our COCO3D benchmark. This metric assesses the consistency of the relative spatial layout between predicted and ground-truth bounding boxes, in the same spirit with the relative depth evaluation [73, 74]. Specifically, we align predicted bounding boxes $\hat{B}$ and ground-truth bounding boxes B by optimizing a global scale factor $s \in \mathbb{R}^+$:

$$s^* = \arg\max_s \frac{1}{N} \sum_{i=1}^{N} \text{IoU}_{\text{3D}}(s \cdot \hat{B}_i, B_i),$$

where N is the total number of boxes. Due to the non-differentiability of IoU_{3D} with respect to s, we perform a grid search within a bounded interval. AP_{3D} and AR_{3D} are then computed on the aligned, scale-normalized predictions, emphasizing relative 3D box layout rather than metric accuracy.

5.2 Main Results

LabelAny3D improves monocular 3D detection on COCO3D. Table 1 benchmarks OVMono3D [75] trained with different datasets. When pretrained solely on Omni3D [7], the model exhibits limited generalization to COCO3D images, likely due to substantial domain gaps. To improve performance, we generate pseudo labels on the MS-COCO [40] training set using the auto-labeling

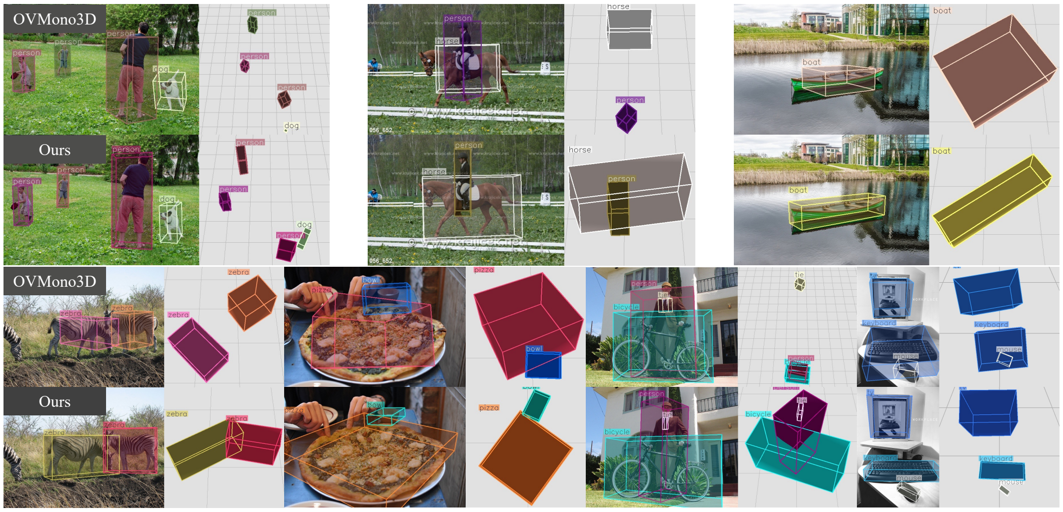

Figure 5: Qualitative open-vocabulary 3D detection results on in-the-wild-images: OVMono3D [75] *vs.* our fine-tuned OVMono3D. We display both the 3D predictions overlaid on the image and a top-down view with a base grid of 1 m × 1 m tiles.

Table 2: Pseudo annotation quality on COCO3D benchmark. The best results for each metric are highlighted in **bold**. "Rel" denotes the relative layout metrics. For fair comparison, we use the same depth for OVM3D-Det as for ours, denoted by "*".

Methods	$\text{AP}_{3\text{D}}\uparrow$	$\text{AP}^{15}_{3\text{D}}\uparrow$	$\text{AP}^{25}_{3\text{D}}\uparrow$	$\text{AP}^{50}_{3\text{D}}\uparrow$	$\text{AR}_{3\text{D}}\uparrow$	$\text{AP}^{\text{Rel}}_{3\text{D}}\uparrow$	$\text{AR}^{\text{Rel}}_{3\text{D}}\uparrow$
OVM3D-Det* [27]	10.03	16.88	9.03	1.44	17.82	10.04	17.84
LabelAny3D	**64.17**	**82.11**	**74.47**	**57.34**	**73.57**	**64.17**	**73.57**

pipeline proposed in OVM3D-Det [27]. However, training OVMono3D from scratch with these labels fails to converge. Even when initialized from the pretrained OVMono3D, fine-tuning on OVM3D-Det labels alone leads to poor performance. When fine-tuned on the combined dataset of Omni3D and OVM3D-Det, the model achieves only a marginal 0.95 $\text{AP}_{3\text{D}}$ gain on COCO3D and shows degraded performance on novel categories, suggesting that excessive label noise negatively impacts learning.

In contrast, training OVMono3D from scratch on pseudo-labels generated by our LabelAny3D exhibits better performance on COCO3D, demonstrating the effectiveness of our pipeline in supporting model training. Notably, the model trained solely on COCO3D pseudo labels achieves 8.47 $\text{AP}_{3\text{D}}$ on OVMono3D's out-of-domain novel categories, highlighting its improved generalizability. Further gains are observed when fine-tuning the pretrained OVMono3D model on the combined Omni3D and LabelAny3D pseudo-labeled datasets, resulting in a 5.05 $\text{AP}_{3\text{D}}$ increase on COCO3D and improved performance across novel categories. These results validate the effectiveness of our LabelAny3D pipeline in producing high-quality, in-the-wild 3D annotations.

Despite these gains, all fine-tuned models show some degradation on OVMono3D's base categories. We attribute this to two factors: (1) increased scene and category diversity without a corresponding increase in model capacity, leading to catastrophic forgetting; and (2) label noise in the pseudo annotations, which may introduce harmful gradients during training.

Figure 5 presents qualitative examples on COCO3D. Compared to the baseline model, our fine-tuned OVMono3D demonstrates stronger detection robustness in diverse scenes, particularly for novel object categories that are underrepresented in existing datasets, such as *animals*, *pizza*, *tie*, *boat*.

LabelAny3D achieves better pseudo annotations. Table 2 compares LabelAny3D with OVM3D-Det [27] on the quality of pseudo annotations. LabelAny3D consistently outperforms the baseline across all reported metrics. The $\text{AP}_{3\text{D}}$ between automatically generated and human-refined annotations is 64.17, indicating minimal manual correction and demonstrating the efficiency of our pipeline. Figure 6 provides a visual comparison with OVM3D-Det [27], revealing the limitations of metric-based priors in in-the-wild settings, where object size and shape vary widely – even within the same category (*e.g.* baby elephants, children, and boats). In such cases, metric depth estimates

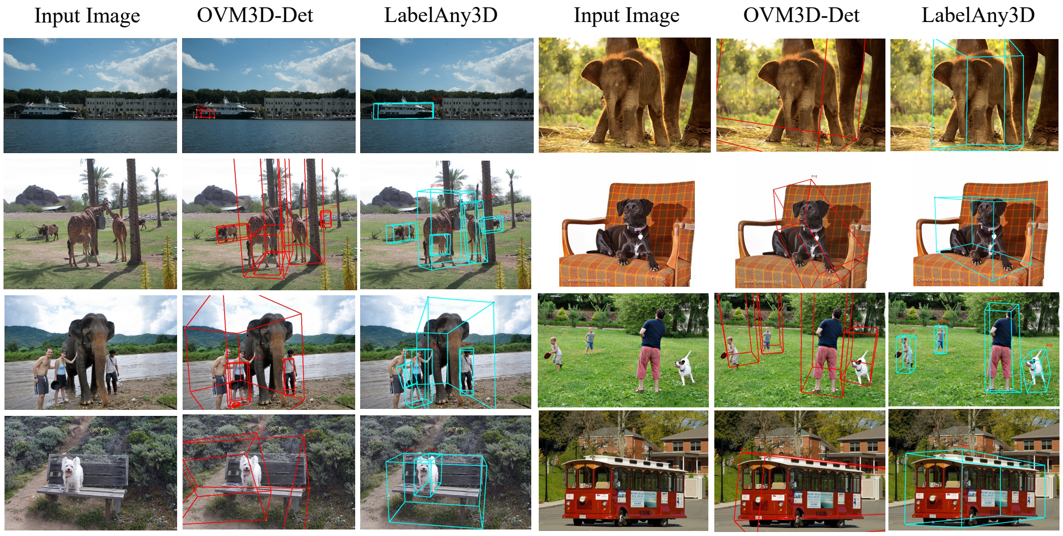

Figure 6: Qualitative comparisons between OVM3D-Det [27] and LabelAny3D *without any human refinement.* These examples illustrate that OVM3D-Det often produces inaccurate metric dimensions for categories with high intra-class size variability, such as humans, animals, vehicles, and furniture.

prone to inaccuracy, leading to misaligned results. In contrast, LabelAny3D leverages relative depth and mesh reconstruction to produce appearance-consistent 3D bounding boxes, resulting in higher annotation fidelity. We further compare the quality of pseudo annotations produced by LabelAny3D and OVM3D-Det [27] on the KITTI [24] benchmark. LabelAny3D achieves a higher overall AP_{3D} of 13.6, compared to 12.39 from OVM3D-Det. Notably, on the truck category, LabelAny3D significantly outperforms OVM3D-Det with an AP_{3D} of 32.74 vs. 13.46, highlighting its effectiveness.

Ablation of components in LabelAny3D. We conduct ablation studies on a subset of the COCO3D dataset and report annotation quality in Table 3. The vanilla 3D scene reconstruction model Gen3DSR [3] achieves an AP_{3D} of only 1.95. In contrast, our full LabelAny3D pipeline achieves a higher AP_{3D} of 43.17. This results shows our pipeline provides better 3D reconstruction for 3D box labeling. Removing the image super-resolution module leads to a substantial drop to 28.13 AP_{3D}, highlighting its importance in enhancing detail for small and distant objects. Eliminating the amodal completion also reduces performance, showing its role to alleviate the negative impact of occlusion.

Table 3: Ablation studies. Default settings are marked in gray .

Framework	AP_{3D} ↑
Gen3DSR [3]	1.95
LabelAny3D	**43.17**
– w/o Super Resolution	28.13
– w/o Amodal Completion	39.22
– w/o MoGe [66]	22.77
– w/ DreamGaussian [64]	36.84
– w/ ICP	24.28

Replacing MoGe's [66] relative depth (scaled to match Depth Pro [6]) with Depth Pro alone leads to a significant drop in performance, showing that MoGe provides more accurate and reliable relative depth. For 3D reconstruction, using TRELLIS [72] improves AP_{3D} by 6.33 points over DreamGaussian [64], suggesting TRELLIS produces more realistic and higher-fidelity reconstructions. To align reconstructed objects with the image point cloud, we compare iterative closest point (ICP) against our used 2D matching + Perspective-n-Point (PnP) method. The latter yields superior results, largely due to the robustness of the underlying 2D matching model.

6 Discussion

In this work, we introduced LabelAny3D, an *analysis-by-synthesis* pipeline for annotating 3D bounding boxes of arbitrary objects from monocular, in-the-wild images. Our pipeline integrates specialized vision foundation models to reconstruct 3D scenes and derive accurate 3D annotations. Leveraging LabelAny3D, we curated COCO3D, a new 3D detection benchmark encompassing diverse object categories beyond existing datasets, with minimal human intervention. Our findings demonstrate that LabelAny3D effectively enhances open-vocabulary 3D detection performance with minimal human effort and enabling the large-scale development of diverse 3D datasets. Our pipeline also has the potential to benefit other 3D scene understanding tasks, such as amodal 3D reconstruction, 6D pose estimation, and scene completion. See supplementary material for implementation details, more qualitative results and analysis.

7 Limitations

While our LabelAny3D pipeline leverages mature foundation models for depth estimation, camera intrinsic estimation, amodal completion, image-to-3D generation, and matching, these models can still fail in challenging scenarios involving heavy occlusion, textureless regions, or small objects, which introduce noise into the final 3D bounding box annotations.

The RGB-to-3D model TRELLIS [72] in our pipeline may generate meshes with ambiguous depth along the viewing direction, causing misalignment with RGBD point clouds and inaccurate bounding boxes. Future work could condition 3D generation on RGBD data, as in Hunyuan3D-Omni [65].

Additionally, future work could investigate robust training strategies for noisy pseudo-annotations.

To ensure benchmark reliability, we exclude objects with erroneous depth estimation, severe occlusion, or truncation. Consequently, our dataset is not exhaustively annotated but can evaluate 2D box-prompted methods like OVMono3D [75] and DetAny3D [78], or end-to-end 3D detection methods using proximity-based metrics.

Since our pipeline integrates depth estimation and amodal completion as modular APIs, future improvements in these components can be directly incorporated to enhance annotation quality. These limitations underscore the need for more robust auto-labeling frameworks and training strategies for open-vocabulary monocular 3D detection.

8 Acknowledgement

The authors acknowledge the University of Virginia Research Computing and Data Analytics Center, Advanced Micro Devices AI and HPC Cluster Program, Advanced Cyberinfrastructure Coordination Ecosystem: Services & Support (ACCESS) program, and National Artificial Intelligence Research Resource (NAIRR) Pilot for computational resources, including the Anvil supercomputer (National Science Foundation award OAC 2005632) at Purdue University and the Delta and DeltaAI advanced computing resources (National Science Foundation award OAC 2005572). This work was supported by Adobe Research Gift, the National Science Foundation (awards 2129824, 2312487, and 2403060), United States Army Research Office (grant W911NF-24-1-0089), and Lockheed Martin Advanced Technology Labs. The authors thank Hao Gu, Guangyi Xu, and Jiahui Zhang for annotation assistance.

References

[1] Josh Achiam, Steven Adler, Sandhini Agarwal, Lama Ahmad, Ilge Akkaya, Florencia Leoni Aleman, Diogo Almeida, Janko Altenschmidt, Sam Altman, Shyamal Anadkat, et al. Gpt-4 technical report. *arXiv preprint arXiv:2303.08774*, 2023. 2, 3

[2] Adel Ahmadyan, Liangkai Zhang, Artsiom Ablavatski, Jianing Wei, and Matthias Grundmann. Objectron: A large scale dataset of object-centric videos in the wild with pose annotations. In *CVPR*, 2021. 2, 3, 7, 24

[3] Andreea Ardelean, Mert Özer, and Bernhard Egger. Gen3dsr: Generalizable 3d scene reconstruction via divide and conquer from a single view, 2025. 4, 9, 26

[4] Gilad Baruch, Zhuoyuan Chen, Afshin Dehghan, Yuri Feigin, Peter Fu, Thomas Gebauer, Daniel Kurz, Tal Dimry, Brandon Joffe, and Arik Schwartz. Arkitscenes: A diverse real-world dataset for 3d indoor scene understanding using mobile rgb-d data. In *NeurIPS*, 2021. 2, 3, 7, 26

[5] Shariq Farooq Bhat, Reiner Birkl, Diana Wofk, Peter Wonka, and Matthias Müller. Zoedepth: Zero-shot transfer by combining relative and metric depth, 2023. 4

[6] Aleksei Bochkovskii, Amaël Delaunoy, Hugo Germain, Marcel Santos, Yichao Zhou, Stephan R Richter, and Vladlen Koltun. Depth pro: Sharp monocular metric depth in less than a second. *arXiv preprint arXiv:2410.02073*, 2024. 2, 3, 4, 9, 23, 26

[7] Garrick Brazil, Abhinav Kumar, Julian Straub, Nikhila Ravi, Justin Johnson, and Georgia Gkioxari. Omni3d: A large benchmark and model for 3d object detection in the wild. In *CVPR*, 2023. 2, 3, 6, 7, 24, 26

[8] Holger Caesar, Varun Bankiti, Alex H Lang, Sourabh Vora, Venice Erin Liong, Qiang Xu, Anush Krishnan, Yu Pan, Giancarlo Baldan, and Oscar Beijbom. nuscenes: A multimodal dataset for autonomous driving. In *CVPR*, 2020. 2, 3, 7, 26

[9] Holger Caesar, Varun Bankiti, Alex H. Lang, Sourabh Vora, Venice Erin Liong, Qiang Xu, Anush Krishnan, Yu Pan, Giancarlo Baldan, and Oscar Beijbom. nuscenes: A multimodal dataset for autonomous driving. In *CVPR*, 2020. 2, 24

[10] Benjamin Caine, Rebecca Roelofs, Vijay Vasudevan, Jiquan Ngiam, Yuning Chai, Zhifeng Chen, and Jonathon Shlens. Pseudo-labeling for scalable 3d object detection. *arXiv preprint arXiv:2103.02093*, 2021. 3

[11] Yang Cao, Zeng Yihan, Hang Xu, and Dan Xu. Coda: Collaborative novel box discovery and cross-modal alignment for open-vocabulary 3d object detection. *NeurIPS*, 2024. 2, 3

[12] Yang Cao, Yihan Zeng, Hang Xu, and Dan Xu. Collaborative novel object discovery and box-guided cross-modal alignment for open-vocabulary 3d object detection. *arXiv preprint arXiv:2406.00830*, 2024. 2, 3

[13] Hansheng Chen, Yuyao Huang, Wei Tian, Zhong Gao, and Lu Xiong. Monorun: Monocular 3d object detection by reconstruction and uncertainty propagation, 2021. 3

[14] Xiaozhi Chen, Kaustav Kundu, Ziyu Zhang, Huimin Ma, Sanja Fidler, and Raquel Urtasun. Monocular 3d object detection for autonomous driving. In *CVPR*, 2016. 3

[15] Angela Dai, Angel X Chang, Manolis Savva, Maciej Halber, Thomas Funkhouser, and Matthias Nießner. Scannet: Richly-annotated 3d reconstructions of indoor scenes. In *CVPR*, 2017. 2

[16] Saumitro Dasgupta, Kuan Fang, Kevin Chen, and Silvio Savarese. Delay: Robust spatial layout estimation for cluttered indoor scenes. In *CVPR*, 2016. 3

[17] Matt Deitke, Dustin Schwenk, Jordi Salvador, Luca Weihs, Oscar Michel, Eli VanderBilt, Ludwig Schmidt, Kiana Ehsani, Aniruddha Kembhavi, and Ali Farhadi. Objaverse: A universe of annotated 3d objects. In *Proceedings of the IEEE/CVF conference on computer vision and pattern recognition*, pages 13142–13153, 2023. 2

[18] Xueqing Deng, Qihang Yu, Peng Wang, Xiaohui Shen, and Liang-Chieh Chen. Coconut: Modernizing coco segmentation, 2024. 4, 25, 26

[19] Carl Doersch, Yi Yang, Dilara Gokay, Pauline Luc, Skanda Koppula, Ankush Gupta, Joseph Heyward, Ross Goroshin, João Carreira, and Andrew Zisserman. Bootstap: Bootstrapped training for tracking-any-point. *arXiv preprint arXiv:2402.00847*, 2024. 3

[20] Djamahl Etchegaray, Zi Huang, Tatsuya Harada, and Yadan Luo. Find n' propagate: Open-vocabulary 3d object detection in urban environments. In *ECCV*, 2024. 2, 3

[21] Martin A Fischler and Robert C Bolles. Random sample consensus: a paradigm for model fitting with applications to image analysis and automated cartography. *Communications of the ACM*, 24(6):381–395, 1981. 5

[22] Yunhao Ge, Hong-Xing Yu, Cheng Zhao, Yuliang Guo, Xinyu Huang, Liu Ren, Laurent Itti, and Jiajun Wu. 3d copy-paste: Physically plausible object insertion for monocular 3d detection. *Advances in Neural Information Processing Systems*, 36:17057–17071, 2023. 2, 3

[23] Andreas Geiger, Philip Lenz, Christoph Stiller, and Raquel Urtasun. Vision meets robotics: The kitti dataset. *The International Journal of Robotics Research*, 32(11):1231–1237, 2013. 2, 3

[24] Andreas Geiger, Philip Lenz, and Raquel Urtasun. Are we ready for autonomous driving? the kitti vision benchmark suite. In *CVPR*, 2012. 2, 7, 9, 26

[25] Andreas Lau Hansen, Lukas Wanzeck, and Dim P. Papadopoulos. Weak cube r-cnn: Weakly supervised 3d detection using only 2d bounding boxes, 2025. 3

[26] Kuan-Chih Huang, Tsung-Han Wu, Hung-Ting Su, and Winston H Hsu. Monodtr: Monocular 3d object detection with depth-aware transformer. In *CVPR*, pages 4012–4021, 2022. 3

[27] Rui Huang, Henry Zheng, Yan Wang, Zhuofan Xia, Marco Pavone, and Gao Huang. Training an open-vocabulary monocular 3d object detection model without 3d data. *arXiv preprint arXiv:2411.15657*, 2024. 2, 3, 5, 7, 8, 9, 23, 24, 26

[28] Siyuan Huang, Siyuan Qi, Yinxue Xiao, Yixin Zhu, Ying Nian Wu, and Song-Chun Zhu. Cooperative holistic scene understanding: Unifying 3d object, layout, and camera pose estimation, 2019. 3

[29] Jitesh Jain, Jiachen Li, Mang Tik Chiu, Ali Hassani, Nikita Orlov, and Humphrey Shi. Oneformer: One transformer to rule universal image segmentation. In *CVPR*, pages 2989–2998, 2023. 3

[30] Hanwen Jiang, Qixing Huang, and Georgios Pavlakos. Real3d: Scaling up large reconstruction models with real-world images. *arXiv preprint arXiv:2406.08479*, 2024. 23

[31] Xueying Jiang, Sheng Jin, Lewei Lu, Xiaoqin Zhang, and Shijian Lu. Weakly supervised monocular 3d detection with a single-view image. In *CVPR*, pages 10508–10518, 2024. 3

[32] Linyi Jin, Richard Tucker, Zhengqi Li, David Fouhey, Noah Snavely, and Aleksander Holynski. Stereo4d: Learning how things move in 3d from internet stereo videos. *arXiv preprint*, 2024. 3

[33] Alexander Kirillov, Eric Mintun, Nikhila Ravi, Hanzi Mao, Chloe Rolland, Laura Gustafson, Tete Xiao, Spencer Whitehead, Alexander C Berg, and Wan-Yen Lo. Segment anything. *arXiv preprint arXiv:2304.02643*, 2023. 2

[34] Alexander Kirillov, Eric Mintun, Nikhila Ravi, Hanzi Mao, Chloe Rolland, Laura Gustafson, Tete Xiao, Spencer Whitehead, Alexander C Berg, and Wan-Yen Lo. Segment anything. In *ICCV*, 2023. 24, 26

[35] Justin Lazarow, David Griffiths, Gefen Kohavi, Francisco Crespo, and Afshin Dehghan. Cubify anything: Scaling indoor 3d object detection. *arXiv preprint arXiv:2412.04458*, 2024. 3

[36] Vincent Lepetit, Francesc Moreno-Noguer, and Pascal Fua. Ep n p: An accurate o (n) solution to the p n p problem. *International journal of computer vision*, 81:155–166, 2009. 5

[37] Vincent Leroy, Yohann Cabon, and Jérôme Revaud. Grounding image matching in 3d with mast3r. In *European Conference on Computer Vision*, pages 71–91. Springer, 2024. 5, 26

[38] Junnan Li, Dongxu Li, Silvio Savarese, and Steven Hoi. Blip-2: Bootstrapping language-image pre-training with frozen image encoders and large language models. In *International conference on machine learning*, pages 19730–19742. PMLR, 2023. 3

[39] Zhuoling Li, Xiaogang Xu, SerNam Lim, and Hengshuang Zhao. Towards unified 3d object detection via algorithm and data unification, 2024. 3

[40] Tsung-Yi Lin, Michael Maire, Serge Belongie, James Hays, Pietro Perona, Deva Ramanan, Piotr Dollár, and C Lawrence Zitnick. Microsoft coco: Common objects in context. In *Computer Vision–ECCV 2014: 13th European Conference, Zurich, Switzerland, September 6-12, 2014, Proceedings, Part V 13*, pages 740–755. Springer, 2014. 2, 3, 4, 5, 6, 7, 25

[41] Tsung-Yi Lin, Michael Maire, Serge Belongie, James Hays, Pietro Perona, Deva Ramanan, Piotr Dollár, and C Lawrence Zitnick. Microsoft coco: Common objects in context. In *ECCV*, 2014. 26

[42] Lahav Lipson, Zachary Teed, and Jia Deng. Raft-stereo: Multilevel recurrent field transforms for stereo matching. In *2021 International Conference on 3D Vision (3DV)*, pages 218–227. IEEE, 2021. 3

[43] Minghua Liu, Chao Xu, Haian Jin, Linghao Chen, Mukund Varma T, Zexiang Xu, and Hao Su. One-2-3-45: Any single image to 3d mesh in 45 seconds without per-shape optimization. *Advances in Neural Information Processing Systems*, 36:22226–22246, 2023. 23, 26

[44] Shilong Liu, Zhaoyang Zeng, Tianhe Ren, Feng Li, Hao Zhang, Jie Yang, Chunyuan Li, Jianwei Yang, Hang Su, and Jun Zhu. Grounding dino: Marrying dino with grounded pre-training for open-set object detection. *arXiv preprint arXiv:2303.05499*, 2023. 2

[45] Shilong Liu, Zhaoyang Zeng, Tianhe Ren, Feng Li, Hao Zhang, Jie Yang, Chunyuan Li, Jianwei Yang, Hang Su, and Jun Zhu. Grounding dino: Marrying dino with grounded pre-training for open-set object detection. *arXiv preprint arXiv:2303.05499*, 2023. 6, 24, 26

[46] Yuheng Lu, Chenfeng Xu, Xiaobao Wei, Xiaodong Xie, Masayoshi Tomizuka, Kurt Keutzer, and Shanghang Zhang. Open-vocabulary 3d detection via image-level class and debiased cross-modal contrastive learning. *arXiv preprint arXiv:2207.01987*, 2022. 2, 3

[47] Yuheng Lu, Chenfeng Xu, Xiaobao Wei, Xiaodong Xie, Masayoshi Tomizuka, Kurt Keutzer, and Shanghang Zhang. Open-vocabulary point-cloud object detection without 3d annotation. In *CVPR*, 2023. 2, 3

[48] Tiange Luo, Chris Rockwell, Honglak Lee, and Justin Johnson. Scalable 3d captioning with pretrained models. *Advances in Neural Information Processing Systems*, 36:75307–75337, 2023. 3

[49] Yinyu Nie, Xiaoguang Han, Shihui Guo, Yujian Zheng, Jian Chang, and Jian Jun Zhang. Total3dunderstanding: Joint layout, object pose and mesh reconstruction for indoor scenes from a single image, 2020. 3

[50] Maxime Oquab, Timothée Darcet, Théo Moutakanni, Huy Vo, Marc Szafraniec, Vasil Khalidov, Pierre Fernandez, Daniel Haziza, Francisco Massa, and Alaaeldin El-Nouby. Dinov2: Learning robust visual features without supervision. *arXiv:2304.07193*, 2023. 6, 24

[51] Liang Peng, Senbo Yan, Boxi Wu, Zheng Yang, Xiaofei He, and Deng Cai. Weakm3d: Towards weakly supervised monocular 3d object detection. *arXiv preprint arXiv:2203.08332*, 2022. 5

[52] Xingyu Peng, Yan Bai, Chen Gao, Lirong Yang, Fei Xia, Beipeng Mu, Xiaofei Wang, and Si Liu. Global-local collaborative inference with llm for lidar-based open-vocabulary detection. In *ECCV*. Springer, 2025. 2, 3

[53] Luigi Piccinelli, Yung-Hsu Yang, Christos Sakaridis, Mattia Segu, Siyuan Li, Luc Van Gool, and Fisher Yu. Unidepth: Universal monocular metric depth estimation. In *Proceedings of the IEEE/CVF Conference on Computer Vision and Pattern Recognition*, pages 10106–10116, 2024. 2, 26

[54] Alec Radford, Jong Wook Kim, Chris Hallacy, Aditya Ramesh, Gabriel Goh, Sandhini Agarwal, Girish Sastry, Amanda Askell, Pamela Mishkin, and Jack Clark. Learning transferable visual models from natural language supervision. In *International conference on machine learning*, pages 8748–8763. PMLR, 2021. 3

[55] Nikhila Ravi, Valentin Gabeur, Yuan-Ting Hu, Ronghang Hu, Chaitanya Ryali, Tengyu Ma, Haitham Khedr, Roman Rädle, Chloe Rolland, and Laura Gustafson. Sam 2: Segment anything in images and videos. *arXiv preprint arXiv:2408.00714*, 2024. 3

[56] Nikhila Ravi, Jeremy Reizenstein, David Novotny, Taylor Gordon, Wan-Yen Lo, Justin Johnson, and Georgia Gkioxari. Accelerating 3d deep learning with pytorch3d. *arXiv preprint arXiv:2007.08501*, 2020. 24

[57] Tianhe Ren, Shilong Liu, Ailing Zeng, Jing Lin, Kunchang Li, He Cao, Jiayu Chen, Xinyu Huang, Yukang Chen, Feng Yan, et al. Grounded sam: Assembling open-world models for diverse visual tasks. *arXiv preprint arXiv:2401.14159*, 2024. 25

[58] Mike Roberts, Jason Ramapuram, Anurag Ranjan, Atulit Kumar, Miguel Angel Bautista, Nathan Paczan, Russ Webb, and Joshua M Susskind. Hypersim: A photorealistic synthetic dataset for holistic indoor scene understanding. In *ICCV*, 2021. 2, 3, 7

[59] Chris Rockwell, Joseph Tung, Tsung-Yi Lin, Ming-Yu Liu, David F Fouhey, and Chen-Hsuan Lin. Dynamic camera poses and where to find them. *arXiv preprint arXiv:2504.17788*, 2025. 3

[60] Robin Rombach, Andreas Blattmann, Dominik Lorenz, Patrick Esser, and Björn Ommer. High-resolution image synthesis with latent diffusion models. In *CVPR*, pages 10684–10695, 2022. 2

[61] Danila Rukhovich, Anna Vorontsova, and Anton Konushin. Imvoxelnet: Image to voxels projection for monocular and multi-view general-purpose 3d object detection, 2021. 3

[62] Andrea Simonelli, Samuel Rota Bulo, Lorenzo Porzi, Manuel López-Antequera, and Peter Kontschieder. Disentangling monocular 3D object detection. In *ICCV*, 2019. 6

[63] Shuran Song, Samuel P Lichtenberg, and Jianxiong Xiao. Sun rgb-d: A rgb-d scene understanding benchmark suite. In *CVPR*, 2015. 2, 3, 7, 24, 26

[64] Jiaxiang Tang, Jiawei Ren, Hang Zhou, Ziwei Liu, and Gang Zeng. Dreamgaussian: Generative gaussian splatting for efficient 3d content creation. *arXiv preprint arXiv:2309.16653*, 2023. 9

[65] Tencent Hunyuan3D Team. Hunyuan3d-omni: A unified framework for controllable generation of 3d assets, 2025. 10

[66] Ruicheng Wang, Sicheng Xu, Cassie Dai, Jianfeng Xiang, Yu Deng, Xin Tong, and Jiaolong Yang. Moge: Unlocking accurate monocular geometry estimation for open-domain images with optimal training supervision. *arXiv preprint arXiv:2410.19115*, 2024. 2, 3, 4, 5, 7, 9, 23, 26

[67] Tai Wang, ZHU Xinge, Jiangmiao Pang, and Dahua Lin. Probabilistic and geometric depth: Detecting objects in perspective. In *Conference on Robot Learning*. PMLR, 2022. 3

[68] Tai Wang, Xinge Zhu, Jiangmiao Pang, and Dahua Lin. Fcos3d: Fully convolutional one-stage monocular 3d object detection, 2021. 3

[69] Zhenyu Wang, Yali Li, Taichi Liu, Hengshuang Zhao, and Shengjin Wang. Ov-uni3detr: Towards unified open-vocabulary 3d object detection via cycle-modality propagation. *arXiv preprint arXiv:2403.19580*, 2024. 3

[70] Yuxin Wu, Alexander Kirillov, Francisco Massa, Wan-Yen Lo, and Ross Girshick. Detectron2. https://github.com/facebookresearch/detectron2, 2019. 24

[71] Zhongyu Xia, Jishuo Li, Zhiwei Lin, Xinhao Wang, Yongtao Wang, and Ming-Hsuan Yang. Openad: Open-world autonomous driving benchmark for 3d object detection. *arXiv preprint arXiv:2411.17761*, 2024. 3

[72] Jianfeng Xiang, Zelong Lv, Sicheng Xu, Yu Deng, Ruicheng Wang, Bowen Zhang, Dong Chen, Xin Tong, and Jiaolong Yang. Structured 3d latents for scalable and versatile 3d generation, 2025. 2, 3, 4, 5, 9, 10, 24, 26

[73] Lihe Yang, Bingyi Kang, Zilong Huang, Xiaogang Xu, Jiashi Feng, and Hengshuang Zhao. Depth anything: Unleashing the power of large-scale unlabeled data. In *CVPR*, pages 10371–10381, 2024. 7

[74] Lihe Yang, Bingyi Kang, Zilong Huang, Zhen Zhao, Xiaogang Xu, Jiashi Feng, and Hengshuang Zhao. Depth anything v2. *arXiv:2406.09414*, 2024. 7

[75] Jin Yao, Hao Gu, Xuweiyi Chen, Jiayun Wang, and Zezhou Cheng. Open vocabulary monocular 3d object detection. *arXiv preprint arXiv:2411.16833*, 2024. 2, 3, 6, 7, 8, 10, 24, 25, 26, 28

[76] Zongsheng Yue, Kang Liao, and Chen Change Loy. Arbitrary-steps image super-resolution via diffusion inversion, 2025. 4, 26

[77] Dongmei Zhang, Chang Li, Renrui Zhang, Shenghao Xie, Wei Xue, Xiaodong Xie, and Shanghang Zhang. Fm-ov3d: Foundation model-based cross-modal knowledge blending for open-vocabulary 3d detection. In *AAAI*, 2024. 2, 3

[78] Hanxue Zhang, Haoran Jiang, Qingsong Yao, Yanan Sun, Renrui Zhang, Hao Zhao, Hongyang Li, Hongzi Zhu, and Zetong Yang. Detect anything 3d in the wild. *arXiv preprint arXiv:2504.07958*, 2025. 2, 3, 10

[79] Hu Zhang, Jianhua Xu, Tao Tang, Haiyang Sun, Xin Yu, Zi Huang, and Kaicheng Yu. Opensight: A simple open-vocabulary framework for lidar-based object detection. In *ECCV*. Springer, 2025. 2, 3

[80] Renrui Zhang, Ziyu Guo, Wei Zhang, Kunchang Li, Xupeng Miao, Bin Cui, Yu Qiao, Peng Gao, and Hongsheng Li. Pointclip: Point cloud understanding by clip. In *CVPR*, 2022. 2, 3

[81] Renrui Zhang, Han Qiu, Tai Wang, Ziyu Guo, Ziteng Cui, Yu Qiao, Hongsheng Li, and Peng Gao. Monodetr: Depth-guided transformer for monocular 3d object detection. In *ICCV*, pages 9155–9166, 2023. 3

[82] Dingfu Zhou, Xibin Song, Yuchao Dai, Junbo Yin, Feixiang Lu, Jin Fang, Miao Liao, and Liangjun Zhang. Iafa: Instance-aware feature aggregation for 3d object detection from a single image, 2021. 3

[83] Xingyi Zhou, Dequan Wang, and Philipp Krähenbühl. Objects as points, 2019. 3

[84] Chenming Zhu, Wenwei Zhang, Tai Wang, Xihui Liu, and Kai Chen. Object2scene: Putting objects in context for open-vocabulary 3d detection. *arXiv preprint arXiv:2309.09456*, 2023. 2, 3

NeurIPS Paper Checklist

1. **Claims**

   Question: Do the main claims made in the abstract and introduction accurately reflect the paper's contributions and scope?

   Answer: [Yes]

   Justification: We clearly state the scope of our work in both the abstract and the introduction. Additionally, we highlight the main contributions of our paper at the end of the introduction.

   Guidelines:

   - The answer NA means that the abstract and introduction do not include the claims made in the paper.
   - The abstract and/or introduction should clearly state the claims made, including the contributions made in the paper and important assumptions and limitations. A No or NA answer to this question will not be perceived well by the reviewers.
   - The claims made should match theoretical and experimental results, and reflect how much the results can be expected to generalize to other settings.
   - It is fine to include aspirational goals as motivation as long as it is clear that these goals are not attained by the paper.

2. **Limitations**

   Question: Does the paper discuss the limitations of the work performed by the authors?

   Answer: [Yes]

   Justification: We mention the limitations of our work in the discussion section and include detailed separate section about the limitations in the Appendix.

   Guidelines:

   - The answer NA means that the paper has no limitation while the answer No means that the paper has limitations, but those are not discussed in the paper.
   - The authors are encouraged to create a separate "Limitations" section in their paper.
   - The paper should point out any strong assumptions and how robust the results are to violations of these assumptions (e.g., independence assumptions, noiseless settings, model well-specification, asymptotic approximations only holding locally). The authors should reflect on how these assumptions might be violated in practice and what the implications would be.
   - The authors should reflect on the scope of the claims made, e.g., if the approach was only tested on a few datasets or with a few runs. In general, empirical results often depend on implicit assumptions, which should be articulated.
   - The authors should reflect on the factors that influence the performance of the approach. For example, a facial recognition algorithm may perform poorly when image resolution is low or images are taken in low lighting. Or a speech-to-text system might not be used reliably to provide closed captions for online lectures because it fails to handle technical jargon.
   - The authors should discuss the computational efficiency of the proposed algorithms and how they scale with dataset size.
   - If applicable, the authors should discuss possible limitations of their approach to address problems of privacy and fairness.
   - While the authors might fear that complete honesty about limitations might be used by reviewers as grounds for rejection, a worse outcome might be that reviewers discover limitations that aren't acknowledged in the paper. The authors should use their best judgment and recognize that individual actions in favor of transparency play an important role in developing norms that preserve the integrity of the community. Reviewers will be specifically instructed to not penalize honesty concerning limitations.

3. **Theory assumptions and proofs**

   Question: For each theoretical result, does the paper provide the full set of assumptions and a complete (and correct) proof?

Answer: [NA]

Justification: The paper highlights on the performance of monocular 3D detection with a new proposed benchmark not including any theoretical assumptions and results.

Guidelines:

- The answer NA means that the paper does not include theoretical results.
- All the theorems, formulas, and proofs in the paper should be numbered and cross-referenced.
- All assumptions should be clearly stated or referenced in the statement of any theorems.
- The proofs can either appear in the main paper or the supplemental material, but if they appear in the supplemental material, the authors are encouraged to provide a short proof sketch to provide intuition.
- Inversely, any informal proof provided in the core of the paper should be complemented by formal proofs provided in appendix or supplemental material.
- Theorems and Lemmas that the proof relies upon should be properly referenced.

4. **Experimental result reproducibility**

Question: Does the paper fully disclose all the information needed to reproduce the main experimental results of the paper to the extent that it affects the main claims and/or conclusions of the paper (regardless of whether the code and data are provided or not)?

Answer: [Yes]

Justification: In the experiments section, we mention all of our settings and data used for model evaluation, pseudo label training and ablation studies following which the mentioned results could be reproduced.

Guidelines:

- The answer NA means that the paper does not include experiments.
- If the paper includes experiments, a No answer to this question will not be perceived well by the reviewers: Making the paper reproducible is important, regardless of whether the code and data are provided or not.
- If the contribution is a dataset and/or model, the authors should describe the steps taken to make their results reproducible or verifiable.
- Depending on the contribution, reproducibility can be accomplished in various ways. For example, if the contribution is a novel architecture, describing the architecture fully might suffice, or if the contribution is a specific model and empirical evaluation, it may be necessary to either make it possible for others to replicate the model with the same dataset, or provide access to the model. In general. releasing code and data is often one good way to accomplish this, but reproducibility can also be provided via detailed instructions for how to replicate the results, access to a hosted model (e.g., in the case of a large language model), releasing of a model checkpoint, or other means that are appropriate to the research performed.
- While NeurIPS does not require releasing code, the conference does require all submissions to provide some reasonable avenue for reproducibility, which may depend on the nature of the contribution. For example
  (a) If the contribution is primarily a new algorithm, the paper should make it clear how to reproduce that algorithm.
  (b) If the contribution is primarily a new model architecture, the paper should describe the architecture clearly and fully.
  (c) If the contribution is a new model (e.g., a large language model), then there should either be a way to access this model for reproducing the results or a way to reproduce the model (e.g., with an open-source dataset or instructions for how to construct the dataset).
  (d) We recognize that reproducibility may be tricky in some cases, in which case authors are welcome to describe the particular way they provide for reproducibility. In the case of closed-source models, it may be that access to the model is limited in some way (e.g., to registered users), but it should be possible for other researchers to have some path to reproducing or verifying the results.

5. **Open access to data and code**

   Question: Does the paper provide open access to the data and code, with sufficient instructions to faithfully reproduce the main experimental results, as described in supplemental material?

   Answer: [Yes]

   Justification: We publicly release our code and data on our project page.

   Guidelines:

   - The answer NA means that paper does not include experiments requiring code.
   - Please see the NeurIPS code and data submission guidelines (https://nips.cc/public/guides/CodeSubmissionPolicy) for more details.
   - While we encourage the release of code and data, we understand that this might not be possible, so "No" is an acceptable answer. Papers cannot be rejected simply for not including code, unless this is central to the contribution (e.g., for a new open-source benchmark).
   - The instructions should contain the exact command and environment needed to run to reproduce the results. See the NeurIPS code and data submission guidelines (https://nips.cc/public/guides/CodeSubmissionPolicy) for more details.
   - The authors should provide instructions on data access and preparation, including how to access the raw data, preprocessed data, intermediate data, and generated data, etc.
   - The authors should provide scripts to reproduce all experimental results for the new proposed method and baselines. If only a subset of experiments are reproducible, they should state which ones are omitted from the script and why.
   - At submission time, to preserve anonymity, the authors should release anonymized versions (if applicable).
   - Providing as much information as possible in supplemental material (appended to the paper) is recommended, but including URLs to data and code is permitted.

6. **Experimental setting/details**

   Question: Does the paper specify all the training and test details (e.g., data splits, hyperparameters, how they were chosen, type of optimizer, etc.) necessary to understand the results?

   Answer: [Yes]

   Justification: We have mentioned experimental setup, data and details used for all processes in experiments section and the implementation details in the supplementary material.

   Guidelines:

   - The answer NA means that the paper does not include experiments.
   - The experimental setting should be presented in the core of the paper to a level of detail that is necessary to appreciate the results and make sense of them.
   - The full details can be provided either with the code, in appendix, or as supplemental material.

7. **Experiment statistical significance**

   Question: Does the paper report error bars suitably and correctly defined or other appropriate information about the statistical significance of the experiments?

   Answer: [No]

   Justification: Due to limited computing resources, we have to limit the possibility of obtaining statistical significance in our experimental results.

   Guidelines:

   - The answer NA means that the paper does not include experiments.
   - The authors should answer "Yes" if the results are accompanied by error bars, confidence intervals, or statistical significance tests, at least for the experiments that support the main claims of the paper.

- The factors of variability that the error bars are capturing should be clearly stated (for example, train/test split, initialization, random drawing of some parameter, or overall run with given experimental conditions).
- The method for calculating the error bars should be explained (closed form formula, call to a library function, bootstrap, etc.)
- The assumptions made should be given (e.g., Normally distributed errors).
- It should be clear whether the error bar is the standard deviation or the standard error of the mean.
- It is OK to report 1-sigma error bars, but one should state it. The authors should preferably report a 2-sigma error bar than state that they have a 96% CI, if the hypothesis of Normality of errors is not verified.
- For asymmetric distributions, the authors should be careful not to show in tables or figures symmetric error bars that would yield results that are out of range (e.g. negative error rates).
- If error bars are reported in tables or plots, The authors should explain in the text how they were calculated and reference the corresponding figures or tables in the text.

8. **Experiments compute resources**

   Question: For each experiment, does the paper provide sufficient information on the computer resources (type of compute workers, memory, time of execution) needed to reproduce the experiments?

   Answer:[Yes]

   Justification: We include the details about the computing resources used for our experiments in the Appendix.

   Guidelines:

   - The answer NA means that the paper does not include experiments.
   - The paper should indicate the type of compute workers CPU or GPU, internal cluster, or cloud provider, including relevant memory and storage.
   - The paper should provide the amount of compute required for each of the individual experimental runs as well as estimate the total compute.
   - The paper should disclose whether the full research project required more compute than the experiments reported in the paper (e.g., preliminary or failed experiments that didn't make it into the paper).

9. **Code of ethics**

   Question: Does the research conducted in the paper conform, in every respect, with the NeurIPS Code of Ethics https://neurips.cc/public/EthicsGuidelines?

   Answer: [Yes]

   Justification: We conform with the NeurIPS Code of Ethics in every aspects.

   Guidelines:

   - The answer NA means that the authors have not reviewed the NeurIPS Code of Ethics.
   - If the authors answer No, they should explain the special circumstances that require a deviation from the Code of Ethics.
   - The authors should make sure to preserve anonymity (e.g., if there is a special consideration due to laws or regulations in their jurisdiction).

10. **Broader impacts**

    Question: Does the paper discuss both potential positive societal impacts and negative societal impacts of the work performed?

    Answer: [Yes]

    Justification: We include potential broader societal impact in the Appendix

    Guidelines:

    - The answer NA means that there is no societal impact of the work performed.

- If the authors answer NA or No, they should explain why their work has no societal impact or why the paper does not address societal impact.
- Examples of negative societal impacts include potential malicious or unintended uses (e.g., disinformation, generating fake profiles, surveillance), fairness considerations (e.g., deployment of technologies that could make decisions that unfairly impact specific groups), privacy considerations, and security considerations.
- The conference expects that many papers will be foundational research and not tied to particular applications, let alone deployments. However, if there is a direct path to any negative applications, the authors should point it out. For example, it is legitimate to point out that an improvement in the quality of generative models could be used to generate deepfakes for disinformation. On the other hand, it is not needed to point out that a generic algorithm for optimizing neural networks could enable people to train models that generate Deepfakes faster.
- The authors should consider possible harms that could arise when the technology is being used as intended and functioning correctly, harms that could arise when the technology is being used as intended but gives incorrect results, and harms following from (intentional or unintentional) misuse of the technology.
- If there are negative societal impacts, the authors could also discuss possible mitigation strategies (e.g., gated release of models, providing defenses in addition to attacks, mechanisms for monitoring misuse, mechanisms to monitor how a system learns from feedback over time, improving the efficiency and accessibility of ML).

11. **Safeguards**

    Question: Does the paper describe safeguards that have been put in place for responsible release of data or models that have a high risk for misuse (e.g., pretrained language models, image generators, or scraped datasets)?

    Answer: [NA]

    Justification: To the best our knowledge, no such risk is associated with the work.

    Guidelines:

    - The answer NA means that the paper poses no such risks.
    - Released models that have a high risk for misuse or dual-use should be released with necessary safeguards to allow for controlled use of the model, for example by requiring that users adhere to usage guidelines or restrictions to access the model or implementing safety filters.
    - Datasets that have been scraped from the Internet could pose safety risks. The authors should describe how they avoided releasing unsafe images.
    - We recognize that providing effective safeguards is challenging, and many papers do not require this, but we encourage authors to take this into account and make a best faith effort.

12. **Licenses for existing assets**

    Question: Are the creators or original owners of assets (e.g., code, data, models), used in the paper, properly credited and are the license and terms of use explicitly mentioned and properly respected?

    Answer: [Yes]

    Justification: The papers of existing code, models and datasets are adequately credited and cited in all sections of the paper. We have reviewed and complied with the licenses of all referenced works. We include a section of licenses of assets used in our supplementary material.

    Guidelines:

    - The answer NA means that the paper does not use existing assets.
    - The authors should cite the original paper that produced the code package or dataset.
    - The authors should state which version of the asset is used and, if possible, include a URL.
    - The name of the license (e.g., CC-BY 4.0) should be included for each asset.

- For scraped data from a particular source (e.g., website), the copyright and terms of service of that source should be provided.
- If assets are released, the license, copyright information, and terms of use in the package should be provided. For popular datasets, paperswithcode.com/datasets has curated licenses for some datasets. Their licensing guide can help determine the license of a dataset.
- For existing datasets that are re-packaged, both the original license and the license of the derived asset (if it has changed) should be provided.
- If this information is not available online, the authors are encouraged to reach out to the asset's creators.

13. **New assets**

    Question: Are new assets introduced in the paper well documented and is the documentation provided alongside the assets?

    Answer: [Yes]

    Justification: We will release all new assets along side proper documentation.

    Guidelines:

    - The answer NA means that the paper does not release new assets.
    - Researchers should communicate the details of the dataset/code/model as part of their submissions via structured templates. This includes details about training, license, limitations, etc.
    - The paper should discuss whether and how consent was obtained from people whose asset is used.
    - At submission time, remember to anonymize your assets (if applicable). You can either create an anonymized URL or include an anonymized zip file.

14. **Crowdsourcing and research with human subjects**

    Question: For crowdsourcing experiments and research with human subjects, does the paper include the full text of instructions given to participants and screenshots, if applicable, as well as details about compensation (if any)?

    Answer: [NA]

    Justification: The paper does not involve crowdsourcing platforms or research with human subjects as defined by ethics review standards. All data annotations were performed internally by co-authors or lab members.

    Guidelines:

    - The answer NA means that the paper does not involve crowdsourcing nor research with human subjects.
    - Including this information in the supplemental material is fine, but if the main contribution of the paper involves human subjects, then as much detail as possible should be included in the main paper.
    - According to the NeurIPS Code of Ethics, workers involved in data collection, curation, or other labor should be paid at least the minimum wage in the country of the data collector.

15. **Institutional review board (IRB) approvals or equivalent for research with human subjects**

    Question: Does the paper describe potential risks incurred by study participants, whether such risks were disclosed to the subjects, and whether Institutional Review Board (IRB) approvals (or an equivalent approval/review based on the requirements of your country or institution) were obtained?

    Answer: [NA]

    Justification: The paper does not involve crowdsourcing or research with human subjects, and therefore does not require IRB or equivalent ethical approval.

    Guidelines:

- The answer NA means that the paper does not involve crowdsourcing nor research with human subjects.
- Depending on the country in which research is conducted, IRB approval (or equivalent) may be required for any human subjects research. If you obtained IRB approval, you should clearly state this in the paper.
- We recognize that the procedures for this may vary significantly between institutions and locations, and we expect authors to adhere to the NeurIPS Code of Ethics and the guidelines for their institution.
- For initial submissions, do not include any information that would break anonymity (if applicable), such as the institution conducting the review.

16. **Declaration of LLM usage**

    Question: Does the paper describe the usage of LLMs if it is an important, original, or non-standard component of the core methods in this research? Note that if the LLM is used only for writing, editing, or formatting purposes and does not impact the core methodology, scientific rigorousness, or originality of the research, declaration is not required.

    Answer: [NA]

    Justification: The study deals with 3D detection for in the wild monocular images leveraging state of the art foundation models, not involving LLMs for any critical operations or experiments.

    Guidelines:

    - The answer NA means that the core method development in this research does not involve LLMs as any important, original, or non-standard components.
    - Please refer to our LLM policy (https://neurips.cc/Conferences/2025/LLM) for what should or should not be described.

Appendix

A Human Refinement Interface

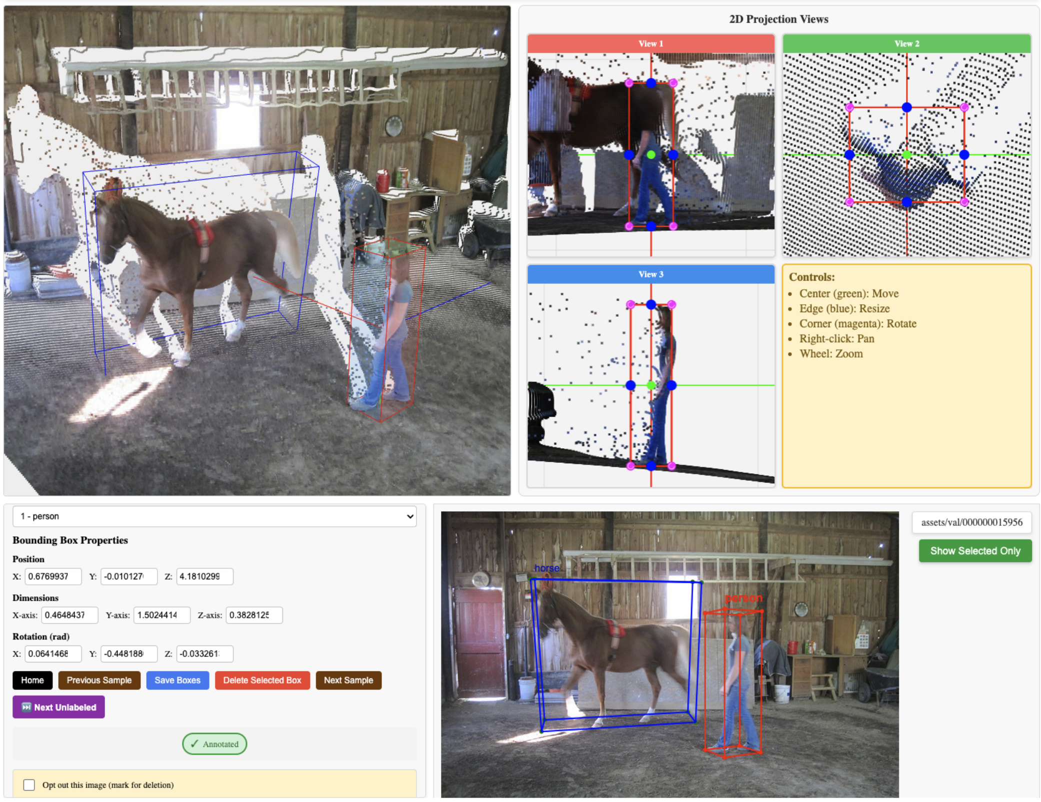

Controls:

- Center (green): Move
- Edge (blue): Resize
- Corner (magenta): Rotate
- Right-click: Pan
- Wheel: Zoom

1 - person

Bounding Box Properties

Position

X: 0.6769937 Y: -0.010127 Z: 4.1810299

Dimensions

X-axis: 0.4648437 Y-axis: 1.5024414 Z-axis: 0.3828125

Rotation (rad)

X: 0.0641468 Y: -0.448188 Z: -0.033261

☐ Opt out this image (mark for deletion)

assets/val/000000015956

Figure 7: Human refinement interface.

Figure 7 illustrates our annotation interface for human refinement of LabelAny3D's automatically generated pseudo labels on COCO3D. The top left panel displays the point cloud and corresponding 3D bounding boxes, which annotators can rotate and translate for an optimal viewing angle. The top-right panel shows three 2D projection views of the point cloud along the local axes of the 3D bounding box. Annotators can adjust the 3D bounding box by manipulating the edges, corners, or center in each view. The lower-left panel shows the attributes of the selected bounding box. Annotators can modify specific parameters (e.g., width) using keyboard shortcuts. They also have the option to delete a bounding box if it corresponds to an invalid 3D object (e.g., a person on a poster). The lower-right panel visualizes the 2D projections of the current 3D boxes to provide additional context. Annotators may also choose to discard the entire image if the relative geometry is incorrect or no valid 3D objects are present.

B Annotation Efficiency

Table 4 presents a category-wise overview of AP_{3D}, AR_{3D}, and average IoU_{3D} for the pseudo annotations generated by LabelAny3D, evaluated against our refined COCO3D benchmark. The results demonstrate that our pipeline produces high-quality annotations with human-like accuracy. In addition to achieving high precision, the average IoU exceeds 0.40 for the majority of categories, indicating strong alignment of spatial layout.

Table 2 compares the overall AP_{3D} of our method against the baseline OVM3D-DET [27], with our approach achieving a higher AP of 64.17. Among the 5,373 annotations in the COCO3D benchmark, 3,146 were accepted by human annotators without modification, while 2,227 required only minor refinement. Just 466 were rejected due to issues such as reflections, 2D object representations, or insufficient point cloud quality.

These results demonstrate that LabelAny3D produces high-quality pseudo annotations that can serve as effective initialization for human annotators. With minimal effort required for refinement, our pipeline significantly reduces manual workload and accelerates the overall annotation process.

Table 4: **Per-category 3D annotation quality for the top 50 categories**. Comparison between pseudo annotations from LabelAny3D and human-refined annotations. Ranking is based on IoU_{3D}.

Category	$\text{AP}_{\text{3D}}\uparrow$	$\text{AR}_{\text{3D}}\uparrow$	$\text{IoU}_{\text{3D}}\uparrow$	Category	$\text{AP}_{\text{3D}}\uparrow$	$\text{AR}_{\text{3D}}\uparrow$	$\text{IoU}_{\text{3D}}\uparrow$
sports ball	81.58	88.26	80.94	bed	88.84	93.33	76.32
fire hydrant	91.14	94.80	75.16	airplane	90.61	93.53	68.83
couch	70.05	88.57	67.89	snowboard	63.50	72.14	68.27
parking meter	92.56	94.29	63.94	mouse	68.98	78.70	63.57
vase	89.89	92.73	61.38	skateboard	69.87	80.73	60.70
fork	64.76	75.65	58.93	cat	72.94	80.49	57.66
bicycle	83.45	94.65	56.60	microwave	82.65	90.53	56.00
dog	79.54	90.36	54.73	tie	48.71	67.83	54.60
bus	84.28	93.61	52.20	dining table	86.38	92.22	51.59
bench	84.80	89.81	49.43	surfboard	50.10	65.00	48.24
sink	60.22	71.95	46.97	sandwich	65.13	77.94	47.38
refrigerator	72.87	86.52	45.04	kite	70.54	80.71	44.99
laptop	69.56	84.69	43.92	cake	80.60	90.40	43.38
oven	66.77	79.05	43.29	umbrella	92.28	95.21	41.30
tv	43.71	62.54	41.10	bowl	79.32	88.40	40.70
horse	76.75	89.84	40.38	bear	82.62	89.71	40.28
backpack	69.39	82.11	38.90	keyboard	47.08	61.82	38.36
pizza	70.90	81.82	37.22	skis	40.44	64.25	36.93
traffic light	62.11	77.12	36.80	cup	89.94	93.44	36.35
remote	59.63	71.60	35.49	tennis racket	38.10	59.31	31.62
clock	39.06	57.36	33.25	elephant	87.71	98.82	33.19
handbag	68.75	82.28	32.23	wine glass	97.11	98.51	31.76
chair	61.75	88.63	32.60	horse	76.75	89.84	40.38
boat	80.06	90.29	12.15	bird	70.48	85.53	16.68
motorcycle	92.65	96.77	13.99	book	65.94	76.75	13.57

C Implementation Details

During annotation, we exclude objects whose masks contain fewer than 400 pixels. Following [30], we also discard objects whose masks overlap the image boundary by more than 10 pixels, treating them as truncated.

For depth estimation, we align the scale-invariant depth map from MoGe [66] with the metric-scale depth map predicted by Depth Pro [6] using a global scale transformation. Specifically, we first use MoGe to generate a relative depth map and extract camera intrinsics. Then, we apply Depth Pro to predict a metric-scale depth map for the same scene. We perform RANSAC-based linear regression to fit a robust scale factor that maps MoGe's relative depths to Depth Pro's metric scale. This allows us to retain the fine geometric details from MoGe while calibrating the scale to real-world distances.

For 2D–3D matching, we first estimate the camera elevation angle using the elevation module from One-2-3-45 [43], based on the amodal-completed object crop. We then render 8 views of the object at the estimated elevation, with azimuths spaced at 45-degree intervals. After computing correspondences between the amodal crop and the 8 rendered views, we obtain an initial camera pose.

Using this pose, we render the mesh again and perform an additional 2D–3D matching step to refine the camera pose. Generating pseudo annotations for a single object takes approximately one minute.

Our implementation is based on PyTorch3D [56] and Detectron2 [70]. Following [75], we use DINOv2-Base [50] as the image feature encoder and freeze its parameters during training. The model is initialized from the publicly released OVMono3D weights and fine-tuned for 58k steps with a batch size of 64. We train the model using SGD with an initial learning rate of 0.0012, which decays by a factor of 10 at 60% and 80% of training. A linear warm-up is applied for the first 1.8k steps. Training takes approximately 48 hours on 4 NVIDIA A40 GPUs. We apply standard image augmentations during training, including random horizontal flipping and resizing. In addition, a random positional perturbation is applied to the input 2D bounding box, with a maximum offset ratio of 0.2. For evaluation on COCO3D, we use ground-truth 2D boxes as input. For Omni3D [7], we adopt the same 2D detections from Grounding DINO [45] as used in OVMono3D [75].

D Labeling Performance on Additional Benchmarks

We compare LabelAny3D with baseline OVM3D-Det [27] on three established benchmarks: SUN-RGBD [63], nuScenes [9], and Objectron [2], covering indoor, self-driving, and object-centric domains, respectively. We randomly sample approximately 300 images from each dataset's test split in Omni3D [7]. Using ground truth 2D boxes as input, we query SAM [34] to obtain instance masks, then generate 3D boxes using both methods.

Since our pipeline filters out small or heavily occluded objects—as TRELLIS [72], the state-of-the-art 3D reconstruction model used in our pipeline, is sensitive to occlusion and object size—we first evaluate performance on highly visible objects. LabelAny3D achieves AP_{3D} of 37.71, 13.59, and 6.07 on SUN-RGBD [63], nuScenes [9], and Objectron [2], respectively, while baseline OVM3D-Det [27] achieves 37.58, 11.38, and 3.84.

On low-visibility objects, LabelAny3D achieves AP_{3D} of 20.20, 6.69, and 2.54, while OVM3D-Det achieves 25.56, 8.50, and 3.85 on the same benchmarks. These results demonstrate that LabelAny3D performs better on low-occlusion objects, as our 3D scene reconstruction yields more accurate boxes. The baseline method excels on low-visibility objects due to its use of metric-scale object size priors. Note that both methods achieve lower performance on Objectron, likely due to inaccurate metric depth estimation for this dataset.

We further ensemble the two methods, using the baseline for low-visibility objects and LabelAny3D for high-visibility objects. The ensembled method achieves AP_{3D} of 30.23, 9.12, and 4.74 on the three benchmarks, compared to 29.89, 8.22, and 3.73 for the baseline alone, demonstrating that the two methods are complementary.

Table 5: **Comparison of COCO3D with Other Benchmarks.** We report a statistical comparison between COCO3D and existing 3D detection benchmarks on their respective test sets. We report the number of images, categories, covered domains, and the distribution of instances across MS-COCO super categories (percentages reported).

Benchmark	# Img	# Cat	Domain	Person	Food	Animal	Vehicle	Kitchen	Furniture	Accessory	Indoor	Sports	Electronic	Outdoor	Appliance
SUN RGB-D	5,050	82	Indoor	0.1	-	-	0.2	6	65.5	8.0	11.8	-	7.8	-	0.5
ARKitScenes	7,610	15	Indoor	-	-	-	-	10.3	80.5	-	3.1	-	4.1	-	2.1
Hypersim	7,690	29	Indoor	-	-	-	-	0.9	37.2	3.6	49.7	-	8.5	-	-
Objectron	9,314	9	Object	-	-	-	3.4	32.4	12.5	20.9	12.8	-	17.9	-	-
KITTI	3,769	8	Driving	12.9	-	-	64.4	-	-	-	-	-	-	22.8	-
nuScenes	6,019	9	Driving	15.8	-	-	63.1	-	-	-	-	-	-	21.1	-
COCO3D	2,039	80	In the Wild	27.9	9.1	10.9	11.0	8.2	4.2	4.6	4.1	4.5	4.0	1.0	2.0

E Comparison of COCO3D with Existing Benchmarks

Table 5 shows a statistical comparison between COCO3D and existing 3D detection benchmarks on their respective test sets. We report the number of images, categories, covered domains, and the distribution of instances across MS-COCO super categories.

Compared to prior benchmarks—which often focus on specific domains such as indoor environments (e.g., SUN RGB-D), object-centric scenes (e.g., Objectron), or self-driving datasets (e.g., KITTI, nuScenes)—COCO3D offers broader coverage across indoor and outdoor everyday scenes. From the super-category perspective, COCO3D uniquely includes categories from *food*, *animal*, and *sports*, which are often absent in existing 3D datasets. In conclusion, our COCO3D benchmark offers a diverse, real-world, and scalable benchmark for advancing the open-vocabulary monocular 3D detection field.

F COCO3D Benchmark Samples

Figure 8 presents additional samples from our human-refined COCO3D benchmark. The results demonstrate that the relative geometry and spatial layout of the scenes and 3D bounding boxes are highly accurate and align well with human perception.

G More Qualitative Comparisons

We report more qualitative comparisons of OVMono3D [75] with our finetuned variant in Figure 9. Trained with additional pseudo-labeled in-the-wild images, our model produces more accurate predictions for challenging object categories such as animals, athletes, and food.

H Failure Case

Figure 10 illustrates several failure cases of LabelAny3D. In highly occluded scenes, such as the cow in Figure 10(a), the amodal completion model fails to reconstruct the full object, resulting in a 3D bounding box that captures only a partial region. As our method relies on ground-truth 2D instance segmentations, it may incorrectly generate 3D boxes for objects that are not physically present in the 3D scene—for example, the person on a television screen in Figure 10(b). Additionally, for crowded scenes, such as in Figure 10(c), the COCO [40, 18] dataset often lacks per-instance segmentation labels. In such cases, instance segmentation models like Grounded SAM [57] also struggle to separate individual objects accurately, causing our method to miss multiple instances.

I Broader Impact

Our work facilitates efficient 3D annotation of objects from any category in diverse, in-the-wild scenes. By integrating the generated pseudo labels, existing open-vocabulary monocular 3D detectors become more robust to out-of-domain categories (e.g., animals), which can enhance the reliability of autonomous systems such as robots and self-driving vehicles, particularly in safety-critical scenarios.

Our dataset is curated from publicly available sources, and therefore does not raise privacy concerns. While our algorithm is category-agnostic and does not introduce explicit bias, the underlying datasets may reflect societal or geographic biases present in the source data. We encourage future work to investigate and mitigate such biases when deploying systems trained on our annotations.

J Licenses

Table 6: Licenses of assets used.

Asset	License
Cube R-CNN [7]	CC-BY-NC 4.0
Grounding DINO [45]	Apache License 2.0
Segment Anything [34]	Apache License 2.0
Unidepth [53]	CC-BY-NC 4.0
MoGe [66]	MIT License
Depth Pro [6]	Apple License (Link)
InvSR [76]	S-Lab License 1.0 (Link)
One-2-3-45 [43]	Apache License 2.0
TRELLIS [72]	MIT License
Gen3DSR [3]	CC-BY 4.0
MASt3R [37]	CC-BY-NC-SA 4.0
OVMono3D [75]	Apache License 2.0
OVM3D-Det [27]	Apache License 2.0
KITTI [24]	CC-BY-NC-SA 3.0 DEED
nuScenes [8]	CC-BY-NC 4.0
SUN RGB-D [63]	MIT License
ARKitScenes [4]	Apple License (Link)
COCO [41]	CC-BY 4.0
COCONut [18]	Apache License 2.0

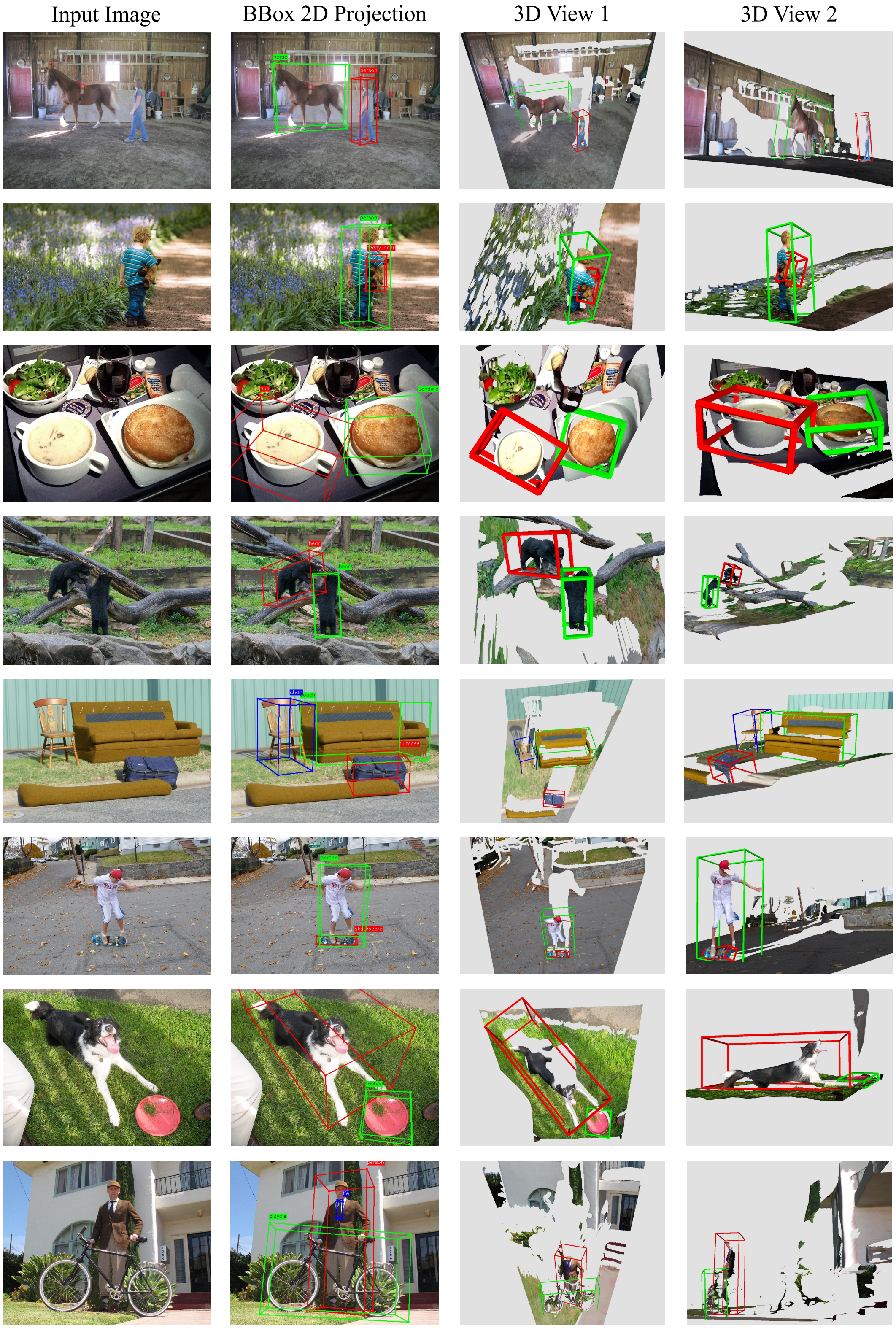

Figure 8: More COCO3D benchmark samples (after human refinement). For each example, we show: (1) the input image, (2) the projected 3D bounding boxes overlaid on the image, and (3–4) two 3D views of the scene point map with the 3D bounding boxes. Please see our project page for rendered videos from 3D Scene and bounding boxes.

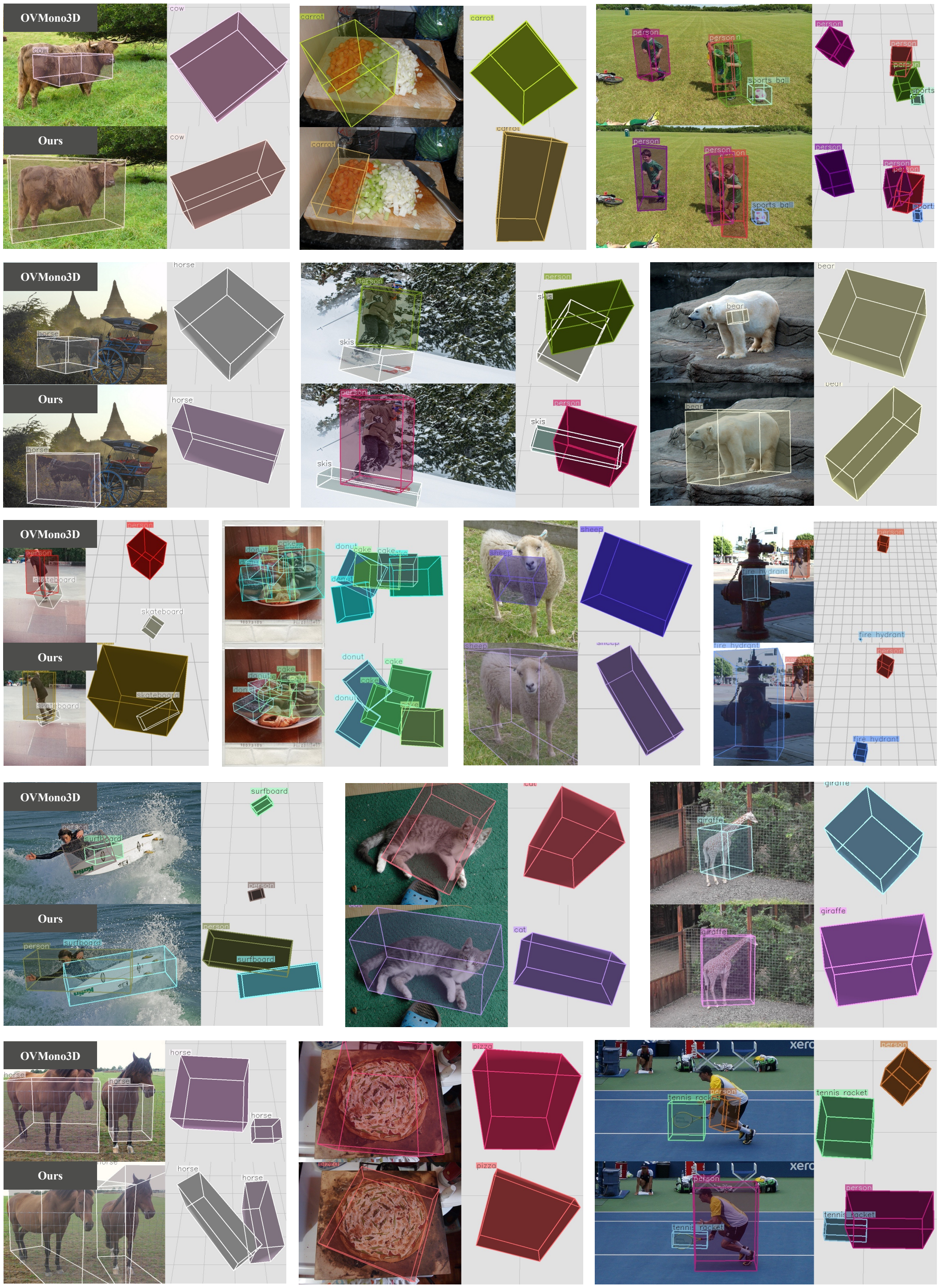

Figure 9: More qualitative open-vocabulary 3D detection results on in-the-wild-images: OVMono3D [75] *vs.* our finetuned OVMono3D. We display both the 3D predictions overlaid on the image and a top-down view with a base grid of 1 m × 1 m tiles.

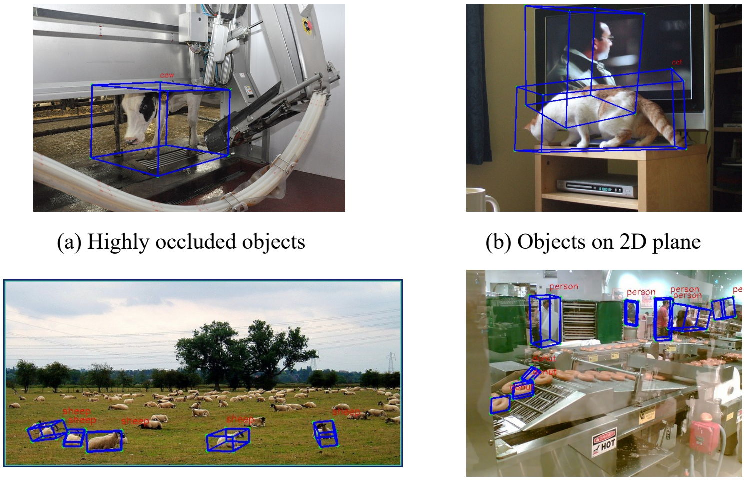

(a) Highly occluded objects

(b) Objects on 2D plane

(c) Too crowded objects

Figure 10: Failure cases.